A Cutter Suction Dredger in waves

Assessment of loading on the structural parts of a Cutter Suction Dredger in waves

by

R.H. de Reus

in partial fulfillment of the requirements for the degree of

Master of Science
in Offshore and Dredging Engineering

at the Delft University of Technology,
to be defended publicly on Monday April 25, 2016 at 09:00.

Thesis committee:	Prof. dr. ir. R. H. M. Huijsmans,	TU Delft
	Ir. J. den Haan,	TU Delft
	Ir. P. de Vos,	TU Delft
	Ir. M. O. Winkelman,	Damen Dredging Equipment

This thesis is confidential and cannot be made public

TU Delft Delft University of Technology

DAMEN

Preface

R.H. de Reus
Delft, April 2016

Dear reader,
In front of you is the final report on Cutter Suction Dredgers (CSDs) of my thesis. This thesis is the deliverable for completing the MSc Offshore & Dredging Engineering at the Delft University of Technology.

Most of the research has been done at the office of Damen Dredging Engineering (DDE), Nijkerk. For almost 14 months I was part of a highly motivated group of people developing, designing and building a very diverse set of dredging tools. However, limited knowledge in the field of hydrodynamics was present at DDE. This made my research a bit more of a challenge but certainly a very satisfying one.

I hope that my work at DDE contributed to the understanding of the workings of CSDs in waves and that the the MATLAB model will be further developed. Understanding of the structural impact of a CSD in waves will almost certainly improve the design of the CSD and lead to a better product and an even more satisfied customer. I am also proud and grateful that Damen offered me the opportunity to start my professional career within the Damen shipyards group.

Acknowledgments

First I would like to thank DDE in general for the facilitation and funding of my research. Within DDE I would like to thank in particular Frank Bosman for getting me on board and Klaas Slager for his extensive knowledge in modeling mathematics and MATLAB. Special thanks go out to Mark Winkelman who has given me the freedom, trust and guidance to do what was needed for this thesis.

From the Technical University of Delft I would like express my gratitude towards professor Huijsmans for chairing the thesis committee. Special thanks go to Joost den Haan for his time, patience, guidance and sometimes a small 'push' in the right direction.

I would also like to acknowledge my sister Lotte de Reus for her help in making the figures in this report as clear as possible and my other sister Liset de Reus for her English spelling checks. And last but not least I would like to give thanks to my parents for their patience and support throughout my studies and other endeavors.

Abstract

The CSD650 is the largest cutter suction dredger produced by Damen Dredging Equipment (DDE) in Nijkerk. To provide for a wider range of clients, the CSD will be used in more coastal conditions. Therefore, it is important to study the behaviour of a cutter suction dredger in waves.

In this context the following research question is formulated: 'What are the operational limits of a CSD650 in waves and, how do harsh environmental conditions affect the important structural parts of a CSD650 over time?' To be able to answer these research questions, the possible failure mechanisms are stated.

Secondly, a linear frequency domain model is build that incorporates all forces acting on the CSD. A twelve degree of freedom model is built in MATLAB and uses DELFRAC potential software to calculate the frequency dependent added mass, damping and wave forces. All the other forces on the CSD are stated as linearized inertia, damping or reaction forces. The ladder of the CSD is treated as a Morison element to calculate the wave forces on the ladder as for the hydrodynamic forces. When the whole equation of the system is known, the equation of motion can be solved to get the Response Amplitude Operators of the system.

Using transformation matrices the RAOs of the centre of gravity of the barge can be transformed to the RAOs of the spud cage. When the mechanical properties of the spud pole and soil interaction are known, the relation between spud motions and stresses can be determined. This relation allows for calculating a stress RAO for the spud pole. In combination with any given wave spectra, so called stress spectra can be determined.

Using the statistical characteristics of these stress spectra, important statistical quantities for the stress response can be derived. Firstly, the probability that a stress cycle amplitude exceeds the yield stress which leads to plastic deformation of the spud pole. With the help of fatigue curves and the Miner rule the fatigue damage, caused by different combinations of significant wave height and peak period, can be calculated with this spectral method. However the model seems to overestimate the values of the fatigue damage and yield stress exceedance probability. It is therefore advised to validate the model with real life measurements.

Figure 1: "the CSD650"

Contents

List of Tables

List of Figures

Nomenclature

A	Area
A_{ws}	Area of wetted surface
C_B	Block factor
C_D	Drag coefficient Morison
C_f	Skin friction coefficient
C_m	Inertia coefficient Morison
$D_{\oslash}$	Diameter
D_{fat}	Fatigue damage
D	Draft
E	Elasticity modulus
F_{nl}	Non linear force
g	Gravitational constant
I_y	Bending moment of inertia in y direction
K	Spring constant
K_s	Size effect
k	Wavenumeber
L_{ij}	Transformation matrix from i to j
L_0	Length in equilibrium
L	Ship Length
m_0	Zeroth spectral moment
m_2	Second spectral moment
M	Moment
n	Number of cycles
N	Number of cycles until failure
P_{nl}	Non linear power
r_e	Effective bilge radius
R_0	Amplitude of roll motion
S_σ	Stress spectrum
S_z	Heave spectrum
S	Wetted surface

v_x	Particle velocity in x direction
x_a	Amplitude of x motion
δl	Elongation
$\Delta\sigma_c$	Detail catagory
ϵ	Strain
ϕ	Phase
∇	Displaced water
ν	Viscosity
ζ	Wave elevation
ω	Angular velocity
ϕ	Pitch
ψ	Yaw
ρ	Volumetric mass
σ	Stress
θ	Roll
θ_{wd}	Wave direction
m_0	Zeroth spectral moment
R_0	Amplitude of roll motion
m_2	Second spectral moment
x_a	Amplitude of x motion
C_B	Block factor
$\Delta\sigma_d$	Constant amplitude fatigue limit
$\Delta\sigma_c$	Detail catagory
$\Delta\sigma_L$	Cut-off limit
$D^*_{\oslash}$	Projected diameter
C_D	Drag coefficient Morison
r_e	Effective bilge radius
D_{fat}	Fatigue damage
C_f	Skin friction coefficient
S_z	Heave spectrum
L_{ij}	Transformation matrix from i to j
δl	Elongation
L_0	Length in equilibrium
C_m	Inertia coefficient Morison

F_{nl}	Non linear force
P_{nl}	Non linear power
K_s	Size effect
S_σ	Stress spectrum
A_{ws}	Area of wetted surface
v_x	Particle velocity in x direction
I_y	Bending moment of inertia in y direction
CSD650	The Damen CSD650
CSD	Cutter Suction Dredger
FD	Frequency domain
GM	Metacentric height
RAO	Response Amplitude Operator
TD	Time domain

1

Introduction

This document is the report of the graduation thesis of Richard de Reus for the Msc Offshore and Dredging Engineering of the TU Delft. The research is be done at and in corporation with Damen Dredging Equipment in Nijkerk the Netherlands. Formerly de Groot Nijkerk became part of the Damen Shipyard group in 1988. But not until 2004 the name was changed in to Damen Dredging Equipment(DDE). DDE makes a range of standardized dredging equipment, including Trailing Suction Hopper Dredgers, Cutter Suction Dredgers, Submersible Dredge Pumps and more.

1.1. Problem Definition

The CSD650 is the biggest CDS produced here in Nijkerk. To provide for a wider range of clients this CDS is certified for coastal area's. This certification heavily influenced the design of the CSD650. However the certification rules are based mainly on seaworthiness and not based on operational limits. Therefore proper investigation of the dynamical behaviour of a CSD650 has never been done at DDE. Due to lack of this investigation the operational limits of the CSD are unknown and it is not sure if the current design of the CSD650 is the most economical. It is thus unsure what the effect of harsh wind wave and current conditions are on the structural parts of the CSD and what these effects are over a long period of operating time. A great opportunity to combine a graduation thesis with added value to DDE.

1.2. Objective

The objective of this research is to gain insight in the behaviour of a CSD in waves and the long time structural effects. This objective is achieved by looking closely at the forces on the dredger for the verification of the design with possible recommendations.

1.3. Thesis Question

"What are the operational limits of a CSD650 in waves and how do harsh environmental conditions effect the important structural parts of an CSD650 over time?"

Through this objective some possible research questions can be formulated.

- What are the operational limits of an CSD650?
- Which sea states lead to these motions and forces?
- What is the fatigue life of a CSD650 in different wave conditions?
- How can the operability be improved from a design point of view?

Approach To be able to answer these research questions a mathematical model is needed to incorporate all forces acting on the CSD. This model must calculate the motions and reaction forces of the suction dredger operating in waves. Although some commercial software is available, it is chosen to develop an algorithm in Matlab. First of all this gives Damen Dredging Equipment the flexibility to develop the algorithm further and apply it to their whole range of CSDs. And second it gives the writer an opportunity to gain in depth knowledge of all the hydrodynamic behaviour of a complex system such as a CSD in the context of the Msc. Offshore and Dredging Engineering. When looking for the limiting forces and motions on a CSD the following parts must be investigated.

- Spud pole
- Spud keeper
- Ladder
- Ladder hinge

1.4. Description of the CSD650

In this section a general description is given about the main case study, the CSD650. Because Damen delivers this type of CSD with many different options these numbers can vary. However the numbers mentioned here are used for further calculation in this study.

Figure 1.1: "The Damen CSD650"

1.4.1. General

General parameters of the CSD650		
Mass	≈	580 Tonnes
length over all (inc. spud keeper)	=	60 m
length over pontoons	=	49.3 m
Beam	=	10 m
Depth	=	2.5 m
Draught	=	1.4 m

Table 1.1: General parameters of the CSD650

1.4.2. Barge and ladder

The numerical value's of the inertia's and masses of the barge and ladder are presented in table 1.2. The numbers are expressed in the units Metric Tonnes and Metric Tonnes per square meter.

Parameters of the CSD650			
Parameter	Barge	Ladder	unit
Mass	520	60	MTonnes
Mass moment of inertia roll	41736	80	Tonnes·m^2
Mass moment of inertia pitch	10442	4000	Tonnes·m^2
Mass moment of inertia yaw	112028	4032	Tonnes·m^2

Table 1.2: Barge and Ladder

The numbers for the ladder are taken from the CSD650 model from ANSYS software. and are taken with respect to the centre of gravity as further clarified in section 3.1.

1.4.3. Segmented spud pole

The spud pole is the most important mooring system that keeps the CSD in place during operations. After arriving at the dredging location the spud is dropped in to the soil to make sure the penetration is deep enough to ensure station keeping.The spud pole is a thin walled tube welded together from multiple sections with different thickness. It's most important feature is its bending stiffness. To account for the different sections a weighted average for the thickness is calculated.

Section	Length [mm]	Fraction of length[-]	Thickness [mm]	Weighted thickness [mm]
1	3000	0.11	35	3.89
2	3000	0.11	40	4.44
3	5400	0.20	35	7.00
4	4600	0.17	32	5.47
5	11000	0.41	19	7.74
Sum	2700	1.00		28.53

Table 1.3: Spud pole

For further calculations a thickness of 28.53 mm is used

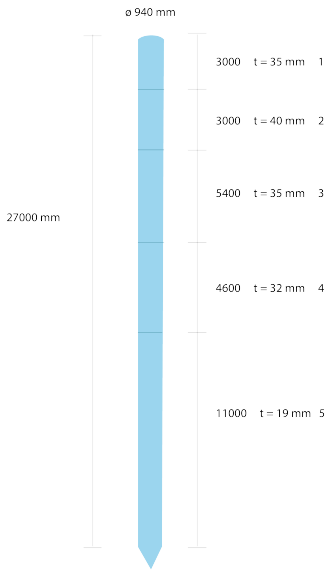

Figure 1.2: "Spud Pole"

1.4.4. Spud keeper

The spud keeper is the part of the CSD that connects the spud pole with the hull of the ship. the spud is able to move freely in the vertical direction. Only the upper and lower spud door guide the vertical forces and moments from the ship to the spud pole and vice versa.

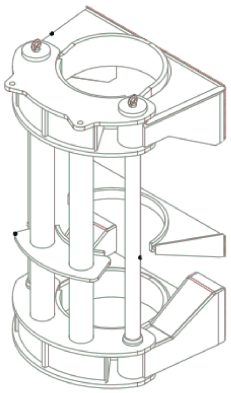

Figure 1.3: "Spud Keeper"

For further purposes the spud and spud keeper are modeled clamped but free sliding in vertical direction as shown below.

Figure 1.4: "Spud keeper model"

1.4.5. Cutter ladder

The cutter ladder is the part of the CSD that connects the cutterhead with the barge. It contains the suction pipe and the sheaves that connect to the A-frame through the hoisting wires. It is also connected to the side wires. These side wires are on one side connected to the anchors that enable the swiveling motion around the spud pole. These motions are powered by the winches on the barge. The motions and forces of the side wires are not taken in to account in this document and model.

Overall length	=	25 m
Centre of gravity from hinge	=	14 m
Hoisting wire from centre of gravity	=	4 m
Mass	=	61.7 Mtonnes
Mass moment of inertia roll	=	80 Ton m^2
Mass moment of inertia Pitch	=	4000 Ton m^2
Mass moment of inertia Yaw	=	4032 ton m^2

Table 1.4: Ladder

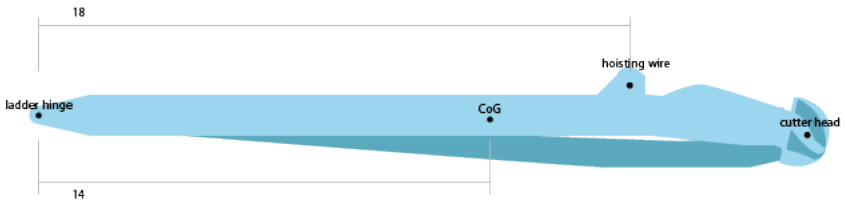

Figure 1.5: ”cutter ladder”

1.5. Operational limits

The operational limits of the CSD are mainly decided by the operator of the CSD. When deciding to abandon operations he must consider the safety, of his own and of his personnel, he must consider the integrity of the dredger and the efficiency of the dredging process.The dangers of on-board personnel could be:

- Water on deck
- Integrity of the dredger
  - Floating pipeline
  - Cutter teeth
  - Spud pole
  - Hoisting wires

  Efficiency of the dredging process
  - Cutter out of the breach
  - Swing motion impossible

2

Failure mechanisms

To investigate the operational limits and to be able to improve the design, various failure mechanisms must first be investigated. Experience learns us that the spud pole is most prone to failure.

2.1. Plastic deformation

When the stress in the out-most fibres of the spud cross-section becomes to large plastic deformation of the spud pole occurs. When the bending moment results in a stress higher than the yield strength of the steel type used. In this case the standard construction steel is uses s355. Which means that is has a yield strength of 355 $\frac{N}{mm^2}$. A highly plastic deformed spud pole can get stuck in the spud cage. The spud can be removed by opening the spud cage door but the spud still must be replaced.

Figure 2.1: ”Deformed spud pole”

2.2. Soil failure

The spud pole is the most important mooring system that the CSD has. This means that when the dredger is not able to maintain its position, the spud pole fails. This is also possible when the soil that the spud pole is subjected to, fails. However due to all the different soil types a dredger can work in, this is outside the scope of this study.

2.3. Pin tube failure

When the spud pole is in the upward position is is maintained in this position by a pin through the spud pole. These pins are guided by a tube from one side to the other 2.2. However when the spud pole is subjected to a perpendicular force, the tube elastically deforms into an oval shape. This results in a high tensile force in the weld of the tubes. When these welds fail the spud is still usable however it will fill with water and be to heavy to lift also the same consequences mentioned in 2.4 will apply.

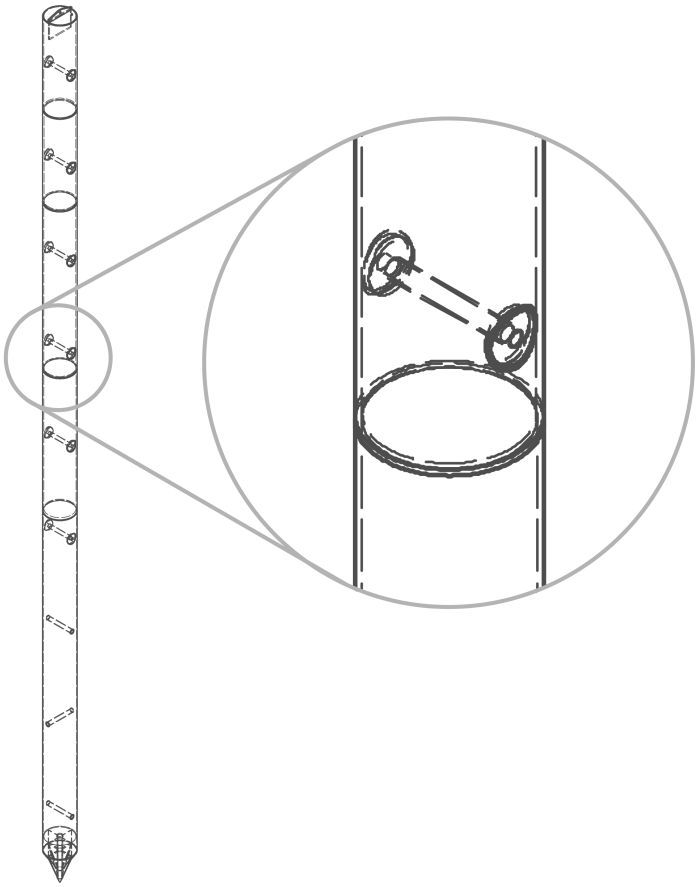

Figure 2.2: ”Spud Pole with Pinholes”

2.4. Segment welds failure

As stated in 1.4.3 the spud pole is divided in 5 different segments. These segments are V-joint but welded together. This means that both segments are only beveled on one side [1]. This results in a v-shaped weld like in in figure 2.3. Due to the fact that this weld can only be performed from the outside of the spud pole one of the main failure mechanisms is that when cracks in the weld appear. When cracks in he weld appear the spud pole might be still usable. However the spud

will fill with water and make hoisting the spud pole either impossible due to the weight increase, or time consuming when waiting for the water to exit at the bottom.

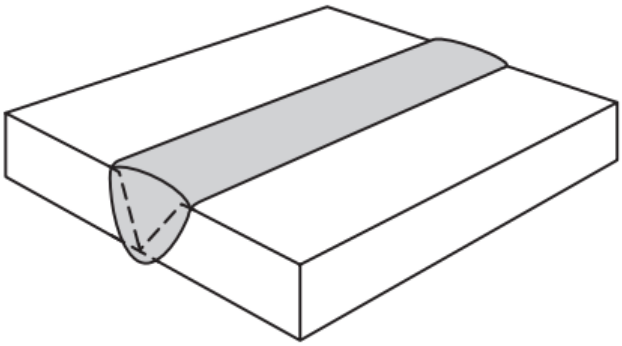

Figure 2.3: ”Single V-shape weld[1]”

3

Model

In this chapter the most important elements of the model will be described. At first a short introduction will be given to clarify the key decisions about the model and especially the overall equation of motion. In section 3.3 all the kinematics that govern the model are described. Then in succession the inertia, drag, spring and coupling terms of the model are discussed. To complete the equation of motion the external forces are treated in section 3.8. Throughout the chapter reference is made to Diffraction theory 3.9 and Morison 3.10.

3.1. Axes

To be able to describe the motions of a CSD in waves in a mathematical sense, and to ensure that motions in one direction do not get confused with another direction, a strict definition of the axes is needed. These axes are conveniently linked with the degrees of freedom of a floating object. These degrees of freedom are:

Degree of freedom	direction / about axis	name	Forces and moments	Linear and angular displacements	Positions and Euler Angles
1	x	Surge	f_x	x	x
2	y	Sway	f_y	y	y
3	z	Heave	f_z	z	z
4	about x	Roll	M_ϕ	ϕ	ϕ
5	about y	Pitch	M_θ	θ	θ
6	about z	Yaw	M_ψ	ψ	ψ

Table 3.1: Definitions

The degrees of freedom from table 3.1 are visualized in figure 3.1.

The conventions in figure 3.2 make the system a 2 mass spring system with 12 degrees of freedom. Three translations and three rotations for the barge and ladder. The motions of these masses are described around their own centres of gravity.

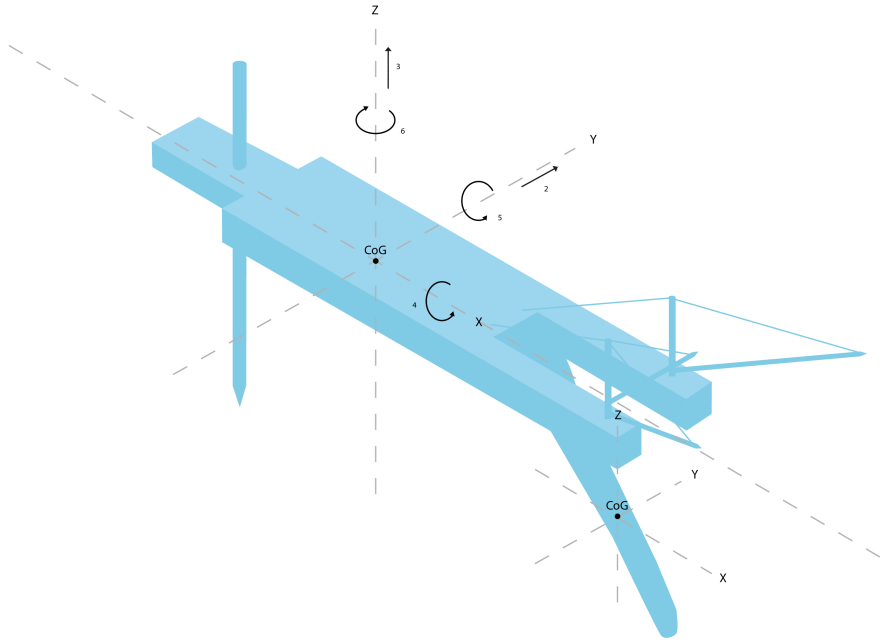

Figure 3.1: ”Degrees of freedom”

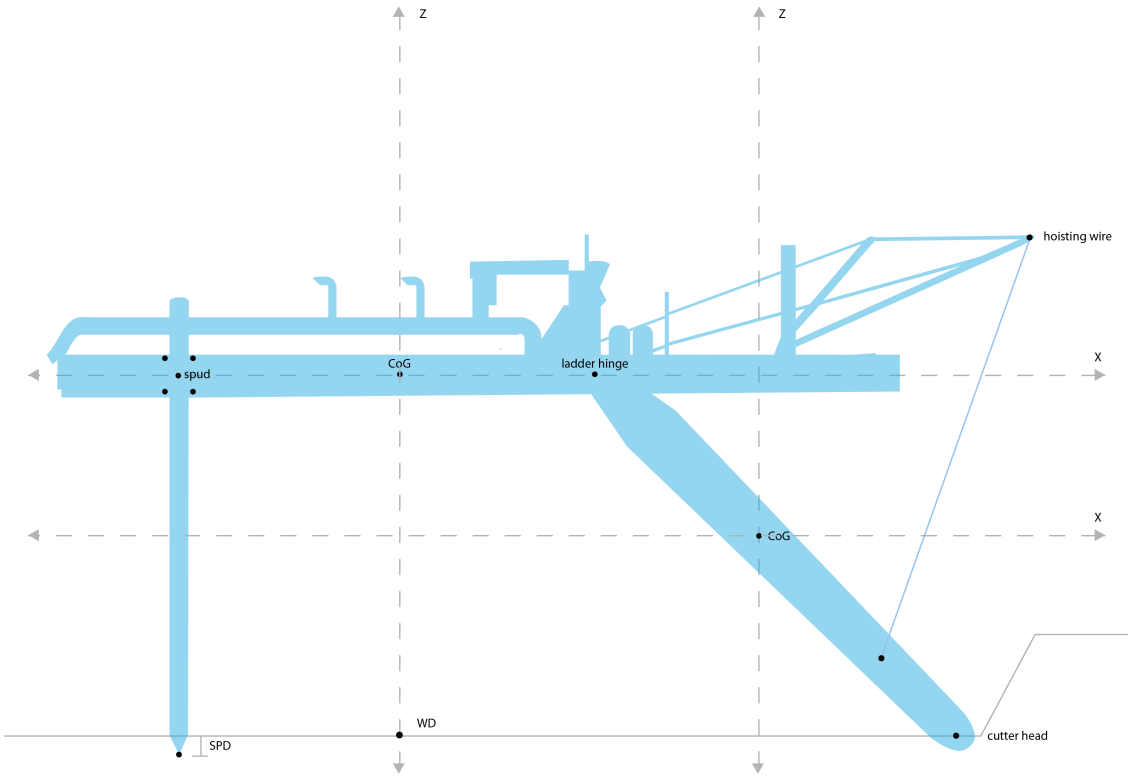

Figure 3.2: ”Axes definition in 2-D”

3.2. Waves

When using potential theory to describe waves it will be necessary to assume that the water surface slope is very small. This means that the wave steepness is so small that terms in the equations of the waves with a magnitude in the order of the steepness-squared can be ignored. Using the linear theory holds here that harmonic displacements, velocities and accelerations of the water particles and also the harmonic pressures will have a linear relation with the wave surface elevation. [2].

$$\eta(t) = A\cos(\omega t + \epsilon) \tag{3.1}$$

This gives a smooth wave shape with;

η = Wave elevation [m]
A = Amplitude of the wave [m]
ω = Angular velocity [rad/s]
t = Time [s]
ϵ = Phase [radians]

However when one looks at the sea at any given moment in time it does not appear to be a harmonic wave. So to get a mathematical description of a 'random' wave one must use the summation of many harmonic waves to create a random sea surface. This is done with randomly chosen amplitudes and phases.

$$\eta(t) = \sum_{i=1}^{N} A_i \cos(\omega_i t + \epsilon_i) \tag{3.2}$$

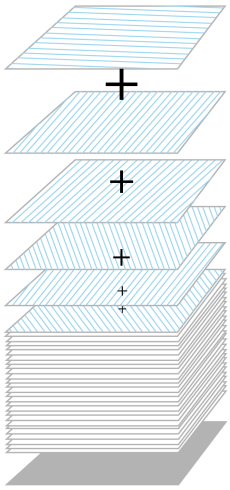

Figure 3.3: "The sum of a large number of harmonic wave components"

3.2.1. Frequencies

To simulate the irregular wave pattern as described in section 3.2 a infinite amount of regular waves would give the best results. However for numerical purposes a finite number of frequencies is needed. The more frequencies are included the better the irregular wave pattern is represented. However for every frequency the calculations must be done. Hence it is key to select the right amount of frequencies to on the one side get a good representation of the wave forces and on the other side avoid unnecessary calculations. The lower limit of the frequency span is 0 radians per second. When a wave is 0 radians per second there is not a wave at all. The upper limit is more a consideration between definition of result and computer time. For this model a

upper limit of 2 radians per second is chosen. This is due to the fact that the waves with higher frequencies than 2 radians per second carry very little energy as seen in wave spectra.5.8 This frequency is divided in 40 different frequencies in this way the energy of the wave spectrum is best represented without losing information.

3.2.2. Directions

Goal of this model is to calculate the effects sea states have on the important elements of the CSD. This means that the input is given as a description of a sea state as a wave spectrum or a scatter diagram. Responses are calculated for 24 wave directions 3.4 and 40 different frequencies. The model must translate this to stress responses for certain parts of the cutter, spud pole, ladder hinge, etc.

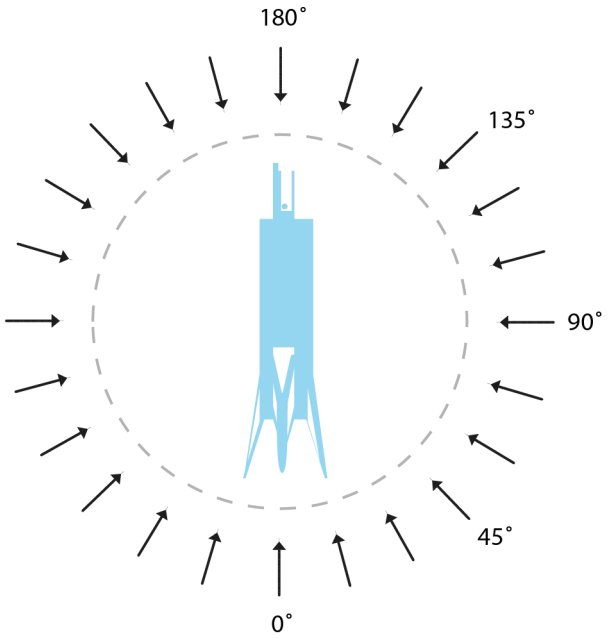

Figure 3.4: "Directions of incoming waves"

3.2.3. Assumptions

In the model several assumptions are made, but the most important are.

- The barge and ladder are considered rigid body's
- Small angles of rotation to maintain linear
- Airy wave theory (inviscid, incompressible and irrotational)

Further assumptions and simplifications are made and are explained throughout the text.

3.2.4. Time vs frequency domain

For the modeling of the cutter suction dredger there are two flavours two chose from. These flavours are the frequency domain and the time domain. The time domain modeling is when the variation of the stress amplitude is calculated over time. In the frequency domain the system is analyzed according to it's response for different frequencies. Frequency domain analysis is more suitable as it enables a long term and and statistical information about the system rather than looking at every individual stress variation. However calculations in the frequency domain must remain linear at all times. However when this assumption holds the calculations remain relatively simple in comparison to the time domain an enables the writer of this document to build the model in MATLAB.

3.2.5. Equation of motion

The equation of motion is based on Newtons law of dynamics, it is given by :

$$m \cdot \ddot{x} = F \tag{3.3}$$

For the system of one degree of freedom is given below:

$$m\ddot{x} = \underbrace{-a_{xx}(\omega) \cdot \ddot{x} - b_{xx}(\omega) \cdot \dot{x}}_{Hydrodynamic\ reaction\ forces} \quad \underbrace{-c_{xx} \cdot x +}_{Restoring\ force} \quad \underbrace{F_{xa} sin(\omega t + \varepsilon_{x\zeta})}_{Wave\ exciting\ force} \tag{3.4}$$

In which:

m	=	Mass of the dredger
$a_{xx}(\omega)$	=	Added mass at frequency ω
$b_{xx}(\omega)$	=	Potential damping at frequency ω
c_{xx}	=	Linear restoring coefficient due to the hydrostatics and the mooring system.
$F_{xa}(\omega)$	=	Amplitude of the steady oscillatory wave exciting force at frequency ω
$\varepsilon_{x\zeta}$	=	Phase angle with regard to wave elevation ζ

3.3. Kinematics

Kinematics is the branch of classical mechanics which describes the motion of points (alternatively "particles"), bodies (objects), and systems of bodies without consideration of the masses of those objects nor the forces that may have caused the motion. [3]

3.3.1. Transformation of displacements

In order to transform the displacements of the centre of gravity to the displacements of any other point within the same rigid body, transformation matrix $\overline{\overline{L}}_{sc}$ is needed and obtained as follows:

$$\begin{bmatrix} x \\ y \\ z \\ \phi \\ \theta \\ \psi \end{bmatrix}_{Spud} = \begin{bmatrix} x \\ y \\ z \\ \phi \\ \theta \\ \psi \end{bmatrix}_{CoG} + \begin{bmatrix} z_{spu}\theta - y_{spu}\psi \\ -z_{spu}\phi + x_{spu}\psi \\ y_{spu}\phi - x_{spu}\theta \\ 0 \\ 0 \\ 0 \end{bmatrix} = \underbrace{\begin{bmatrix} 1 & 0 & 0 & 0 & z_{spu} & -y_{spu} \\ 0 & 1 & 0 & -z_{spu} & 0 & x_{spu} \\ 0 & 0 & 1 & y_{spu} & -x_{spu} & 0 \\ 0 & 0 & 0 & 1 & 0 & 0 \\ 0 & 0 & 0 & 0 & 1 & 0 \\ 0 & 0 & 0 & 0 & 0 & 1 \end{bmatrix}}_{\overline{\overline{L}}_{sc}} \begin{bmatrix} x \\ y \\ z \\ \phi \\ \theta \\ \psi \end{bmatrix}$$

Please note that only small rotations are considered as an example the transformation to the spud is used.

$$\overline{x}_{spud} = \overline{\overline{L}}_{sc}\, \overline{x}_{CoG} \tag{3.5}$$

Figure 3.5: "Transformation of displacements"

3.3.2. Virtual work

The principle of virtual work with deformable bodies is that the virtual work is the same as the virtual change in strain energy. It is often stated as that, external virtual work is equal to internal virtual work when forces and stresses in equilibrium undergo unrelated but consistent displacements and strains. In this next example the principle of virtual work is used to get the K matrix of a wire working between to points a and b, r is the vector of this wire and l_0 is the length of the wire in equilibrium. e_x is the unit vector. The internal virtual work = external virtual work [4]

$$\delta\overline{x}^T \overline{f} = \delta\overline{\epsilon}^T \sigma \tag{3.6}$$

$$\overline{B} = \left[-\frac{\overline{r}\cdot\overline{e}_x}{l_0} \quad 0 \quad -\frac{\overline{r}\cdot\overline{e}_z}{l_0} \quad \frac{\overline{r}\cdot\overline{e}_x}{l_0} \quad 0 \quad \frac{\overline{r}\cdot\overline{e}_z}{l_0}\right] \tag{3.7}$$

$\overline{B}$ is the relationship between the displacements of the points and the strain. The displacements of the two points are;

$$\overline{x} = \begin{bmatrix} x_{hob} \\ y_{hob} \\ z_{hob} \\ x_{hol} \\ y_{hol} \\ z_{hol} \end{bmatrix}$$

Hence

$$\overline{\epsilon} = \overline{B} \cdot \overline{x}$$

Virtual work done by the strain

$$\delta\epsilon = \overline{B}\delta\overline{x}$$

$$\delta\epsilon^T = \delta\overline{x}^T\overline{B}^T$$

Transposed to be substituted in to equation 3.6.

$$\delta\overline{x}^T\overline{f} = \delta\overline{\epsilon}^T\sigma = \delta\overline{x}^T\overline{B}^T S\overline{B}\overline{x}$$

$$\delta\overline{x}^T\overline{f} = \delta\overline{x}^T\overline{B}^T\overline{\overline{S}\overline{B}}^T\overline{x}$$

Since the spring constant is defined as;

$$\overline{f} = \overline{\overline{K}}\overline{x}$$

Hence;

$$\overline{\overline{K}} = \overline{B}^T\overline{\overline{S}\overline{B}}^T$$

3.3.3. Checking the virtual work with the transformation of forces

In order to transform the forces that act on the spud keeper tot the centre of gravity, the transposed matrix of $\overline{\overline{L}}_{sc}$ is needed.

$$\overline{f}_{CoG} = \begin{bmatrix} f_x \\ f_y \\ f_z \\ K \\ M \\ N \end{bmatrix}_{CoG} = \begin{bmatrix} 1 & 0 & 0 & 0 & 0 & 0 \\ 0 & 1 & 0 & 0 & 0 & 0 \\ 0 & 0 & 1 & 0 & 0 & 0 \\ 0 & -z_{spu} & y_{spu} & 1 & 0 & 0 \\ z_{spu} & 0 & -x_{spu} & 0 & 1 & 0 \\ -y_{spu} & x_{spu} & 0 & 0 & 0 & 1 \end{bmatrix} \begin{bmatrix} f_x \\ f_y \\ f_z \\ K \\ M \\ N \end{bmatrix}_{spu}$$

$$\overline{f}_{CoG} = \overline{\overline{L}}_{sc}^T\overline{f}_{spud} \tag{3.8}$$

3.3.4. Check

In order to transform the forces that act on the spud keeper tot the centre of gravity, the transposed matrix of $\overline{\overline{L}}_{sc}$ is needed.

$$\overline{f}_{CoG} = \begin{bmatrix} f_x \\ f_y \\ f_z \\ K \\ M \\ N \end{bmatrix}_{CoG} = \begin{bmatrix} 1 & 0 & 0 & 0 & 0 & 0 \\ 0 & 1 & 0 & 0 & 0 & 0 \\ 0 & 0 & 1 & 0 & 0 & 0 \\ 0 & -z_{spu} & y_{spu} & 1 & 0 & 0 \\ z_{spu} & 0 & -x_{spu} & 0 & 1 & 0 \\ -y_{spu} & x_{spu} & 0 & 0 & 0 & 1 \end{bmatrix} \begin{bmatrix} f_x \\ f_y \\ f_z \\ K \\ M \\ N \end{bmatrix}_{spu}$$

$$\overline{f}_{CoG} = \overline{\overline{L}}_{sc}^T\overline{f}_{spud} \tag{3.9}$$

3.3.5. Tansformation of stiffness matrix

In the equation of motion all the forces are considered in the centre of gravity this is why the stiffness matrix derived from the spud pole must be transformed to a stiffness matrix acting on the CoG.

$$\bar{f}_{spud} = \bar{\bar{K}}_{spud} \cdot \bar{x}_{spud}$$

$$\bar{x}_{spud} = \begin{bmatrix} x \\ y \\ z \\ \phi \\ \theta \\ \psi \end{bmatrix}$$

$$\bar{x}_{spud}^T = \begin{bmatrix} x & y & z & \phi & \theta & \psi \end{bmatrix}$$

To derive the stiffness matrix of the spud pole translated to the CoG the energy relation of a spring is used. Work done by a linear spring is $\frac{1}{2}$·distance · force. In the case of the spud pole this is:

$$\frac{1}{2} \cdot \bar{x}_{spud}^T \cdot \bar{f}_x \tag{3.10}$$

with

$$\bar{f}_x = \bar{\bar{K}}_{spud} \cdot \bar{x}_{spud} \tag{3.11}$$

Substitute in to 3.10.

$$\frac{1}{2} x_{spud}^T \cdot \bar{\bar{K}}_{spud} \cdot \bar{x}_{spud} \tag{3.12}$$

with

$$\bar{x}_{spud} = \bar{\bar{L}}_{sc} \cdot \bar{x}_{CoG}$$

The transposed of a multiplication is the multiplication of the transposed.

$$\bar{x}_{spud}^T = (\bar{\bar{L}}_{sc} \cdot \bar{x}_{CoG})^T = \bar{\bar{L}}_{sc}^T \cdot \bar{x}_{CoG}^T$$

Combinding equation 3.10 and 3.11.

$$\frac{1}{2} \bar{x}_{CoG}^T \cdot \underbrace{\bar{\bar{L}}_{sc}^T \cdot \bar{\bar{K}}_s \cdot \bar{\bar{L}}_{sc}}_{\bar{\bar{K}}_{sc}} \cdot \bar{x}_{CoG}$$

Hence

$$\bar{\bar{K}}_{spud,CoG} = \bar{\bar{L}}_{sc}^T \cdot \bar{\bar{K}}_{sc} \cdot \bar{\bar{L}}_{sc}$$

3.4. Inertia

The equation of motion is basically the balancing of forces over time or frequency. For an object to accelerate a force is needed. This connection is made by Newtons second law, force is the objects mass times its acceleration.

$$F = M \cdot a \tag{3.13}$$

In this section all the inertia terms of the equation of motion are treated. This means all the terms that are multiplied with the acceleration to get a force.

3.4.1. Barge

The mass matrix of the barge looks as follows:

$$\begin{bmatrix} m & 0 & 0 & 0 & 0 & 0 \\ 0 & m & 0 & 0 & 0 & 0 \\ 0 & 0 & m & 0 & 0 & 0 \\ 0 & 0 & 0 & I_{xx} & 0 & 0 \\ 0 & 0 & 0 & 0 & I_{yy} & 0 \\ 0 & 0 & 0 & 0 & 0 & I_{zz} \end{bmatrix}$$

m = Mass of the dredger
I_{xx} = $\int \rho(y^2 + z^2)dA$
I_{yy} = $\int \rho(x^2 + z^2)dA$
I_{zz} = $\int \rho(x^2 + y^2)dA$

Numeric values the numeric values for the ladder mass are:

m	=	520	t
I_{xx}	=	4173	$t \cdot m^2$
I_{yy}	=	10442	$t \cdot m^2$
I_{zz}	=	112030	$t \cdot m^2$

Added mass

In fluid mechanics, added mass or virtual mass is the inertia added to a system because an accelerating or decelerating body must move (or deflect) some volume of surrounding fluid as it moves through it. This mass, that is added to the mass of the moving body, is calculated with diffraction software treated in section 3.10. The added mass is different for every degree of freedom and for every frequency of oscillation.

3.4.2. Ladder

The mass matrix of the ladder is in principle the same as the mass matrix of the barge with different numeric values. However the added mass is calculated with a simpler approach. For the added mass the Morison equation is used.

Numeric values the numeric values for the ladder mass are:

m	=	62 t	
I_{xx}	=	80	$t \cdot m^2$
I_{yy}	=	4000	$t \cdot m^2$
I_{zz}	=	4032	$t \cdot m^2$

Added mass with Morison The added mass of the ladder is calculated with Morison 3.10. For the inertia term a linearisation step is not needed. In the model the translations are calculated with

$$\overline{F}_{in} = \int_{-z}^{z} \frac{\pi}{4}\rho \begin{bmatrix} D^* \\ D \\ D^* \end{bmatrix}^2 C_M \begin{bmatrix} \ddot{x} \\ \ddot{y} \\ \ddot{z} \end{bmatrix} dz \tag{3.14}$$

and for the rotations the calculation is somewhat complicated. For every part of the ladder the velocity relative to the water particles are different and the same rules do not apply to every rotation. For example with roll. This is a motion about the x axis. if $\ddot{\phi}$ = 1 rad/s^2 then the

absolute acceleration in the x_{hinge} and x_{cutter} are the same as the x coordinate due to the 45 degrees ladder angle.

$$\overline{F}_{in} = \int_{-z}^{z} \frac{\pi}{4} \rho D^2 C_M \begin{bmatrix} \ddot{\phi} \\ \ddot{\theta} \\ \ddot{\psi} \end{bmatrix} dz \tag{3.15}$$

3.5. Damping

In this section all the damping terms of the equation of motion are discussed. This means all the terms that are multiplied with the velocity to get a force. These terms are called damping coefficients.

3.5.1. Barge

Potential damping

When a object oscillates in still water, waves are created that travel from the object outwards. These waves take energy out of the oscillating object. This type of energy dissipation is called potential damping or free surface wave damping. This damping is dependent of the frequency of the oscillation and for every degree of freedom different. To determining these coefficients diffraction software is used, this software is clarified more in section 3.9

Viscous roll damping

Due to the fact that potential software does not take viscous effects in to account the damping coefficient for roll damping is underestimated. The damping due to viscous effects must be added to the already calculated damping coefficient by the potential software. Chakrabarti [2001] [5] suggest an empirical calculation method which is used below.

$$B_{total} = B_f + B_e + B_w + B_L + B_{BK} \tag{3.16}$$

in which:

B_f	=	Hull friction damping
B_e	=	Hull eddy shedding damping
B_w	=	Free surface wave damping
B_L	=	Lift force damping
B_{BK}	=	Bilge keel damping

For the case of the CSD, there is no forward speed hence $B_L = 0$. There is no bilge keel hence $B_{BK} = 0$. And the free surface wave damping is already calculated by the potential software.

$$B_f = \frac{4}{3 \cdot \pi} \rho S r_e^3 R_0 C_f \omega \tag{3.17}$$

Where S is the wetted surface calculated with:

$$S = L(1.7D + C_B D) \tag{3.18}$$

ρ is the density of the water in which the friction coefficient Cf is given by:

$$C_f = 1.328 \left[\frac{2\pi\nu}{3.22 r_e^2 R_0^2 \omega} \right]^{\frac{1}{2}} \tag{3.19}$$

With the effective bilge radius is computed from:

$$r_e = \frac{1}{\pi} \left[(0.887 + 0.145 C_B) \frac{S}{L} - 2OG \right] \tag{3.20}$$

R_0 is the amplitude of the roll motion. However this amplitude is only known when the viscous roll damping is already calculated. For the first calculations a roll amplitude of 5 degrees is estimated. However after multiple iteration steps the final value for R_0 is 30 degrees. OG is in this case the same as the draft of the ship.

For the eddy shedding damping coefficient:

$$B_e = \frac{2}{\pi}\rho L D^4 (H_0^2 + 1 - OG/D)[H_0^2 + (1 - OG/D)^2]R_0\omega) \tag{3.21}$$

$$H_0 = \frac{B}{2 \cdot D} \tag{3.22}$$

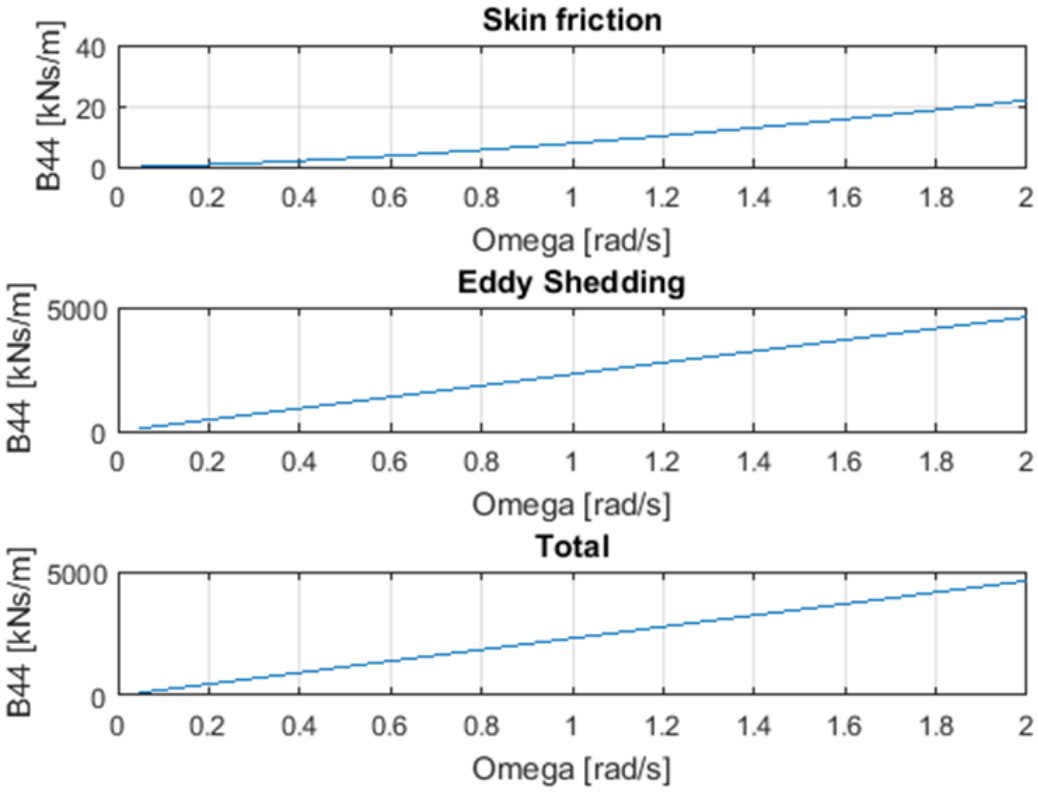

Figure 3.6: ”viscous roll damping”

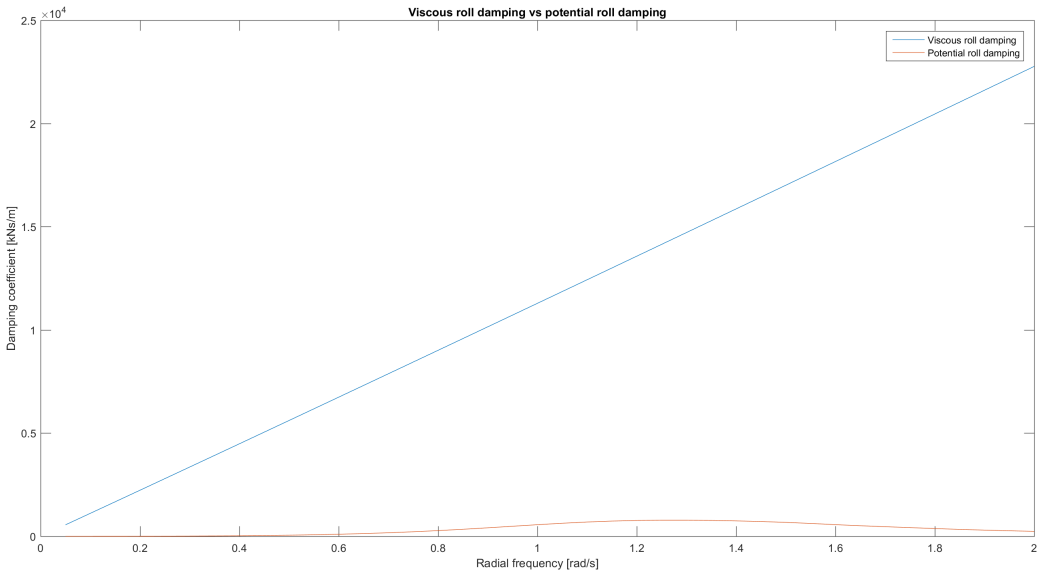

Figure 3.7: ”Potential vs viscous roll damping”

3.5.2. Ladder

To calculate the total force on the ladder the Morison force must be integrated of the length of the ladder. In the following calculations a linearized form of the Morison equation is used. For the linearisation steps the reader referred to section 3.10.2 For the three translations:

$$\overline{F}_{drag,lin} = \int_{-z}^{z} \frac{1}{2}\rho D C_d [\frac{8}{3\pi} \begin{bmatrix} x_a \\ y_a \\ z_a \end{bmatrix}] \begin{bmatrix} \dot{x} \\ \dot{v} \\ \dot{w} \end{bmatrix} dz \tag{3.23}$$

For the three rotations:

$$\overline{F}_{drag,lin} = \int_{-z}^{z} \frac{1}{2}\rho D C_d [\frac{8}{3\pi} \begin{bmatrix} \phi_a \\ \theta_a \\ \psi_a \end{bmatrix}] \begin{bmatrix} \dot{\phi} \\ \dot{\theta} \\ \dot{\psi} \end{bmatrix} /(distancetoCoG) dz \tag{3.24}$$

where the index a means amplitude of the motion.

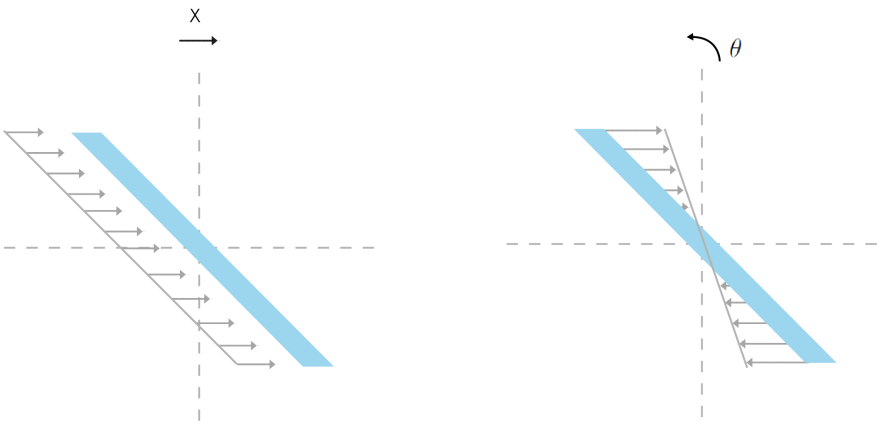

Figure 3.8: "Morison in still water"

The drag force over the length of the spud is:

$$\overline{F}_{drag,lin} = \int_{-z}^{z} \frac{1}{2}\rho D C_d [\frac{8}{3\pi} u_a] \begin{bmatrix} \dot{x} \\ \dot{v} \\ \dot{w} \\ \dot{\phi} \\ \dot{\theta} \\ \dot{\psi} \end{bmatrix} z dz \tag{3.25}$$

3.6. Spring

In this section all the spring terms of the equation of motion are treated. This means all the terms that are multiplied with the displacement to get a force. These terms are called spring coefficients. First the spring terms working on the barge are discussed and then the spring terms of the ladder.

3.6.1. Barge

Hydrostatics

The most important spring term of the barge are the hydrostatics. Due to the hydrostatic forces the barge is floating, upright and stable. In heave direction the spring term is determined with Archimedes law.

$$F = \rho g A_{ws} \cdot \Delta z \tag{3.26}$$

$$K_{hyd,11} = \rho g A_{ws} \tag{3.27}$$

For surge and sway no restoring forces exist. For roll and pitch the restoring forces are calculated with use of the following parameters

KG	=	Distance from keel to centre of gravity
KB	=	Distance from keel to centre of buoyancy
Iy	=	Bending moment of inertia of the water cutting surface in y direction
Ix	=	Bending moment of inertia of the water cutting surface in x direction

$$BM = \frac{I_y}{\nabla} \tag{3.28}$$

$$GM = KB + BM - KG \tag{3.29}$$

$$k_{hyd,44} = \rho g \nabla \cdot GM_x \tag{3.30}$$
$$k_{hyd,55} = \rho g \nabla \cdot GM_y \tag{3.31}$$

Spud

In next section the stiffness matrix of the spud pole is determined. It is assumed that the spud pole is prismatic and it is considered to be clamped in the soil.

$$\overline{f}_{spud} = \overline{\overline{K}}_{spud} \overline{x}_{spud}$$

The displacement and rotation of the spud pole are:

$$u = \frac{f_x l^3}{3EI} + \frac{Ml^2}{2EI}$$
$$\theta = \frac{f_x l^2}{2EI} + \frac{Ml}{EI} = 0$$

In matrix notation this gives:

$$\begin{bmatrix} u \\ \theta \end{bmatrix} = \frac{1}{EI} \begin{bmatrix} \frac{l^3}{3} & \frac{l^2}{2} \\ \frac{l^2}{2} & \frac{l}{1} \end{bmatrix} \begin{bmatrix} f_x \\ M \end{bmatrix}$$

$$\begin{bmatrix} f_x \\ M \end{bmatrix} = \frac{12EI}{l^4} \begin{bmatrix} l & -\frac{l^2}{2} \\ -\frac{l^2}{2} & \frac{l^3}{3} \end{bmatrix} \begin{bmatrix} x \\ \theta \end{bmatrix}$$

$$= \frac{EI}{l^3} \begin{bmatrix} 12 & -6l \\ -6l & 4l^2 \end{bmatrix} \begin{bmatrix} x \\ \theta \end{bmatrix}$$

$$\begin{bmatrix} f_x \\ f_z \\ M \end{bmatrix} = \underbrace{\frac{EI}{l^3} \begin{bmatrix} 12 & 0 & -6l \\ 0 & 0 & 0 \\ -6l & 0 & 4l^2 \end{bmatrix}}_{\overline{\overline{K}}_{spud}} \begin{bmatrix} u \\ w \\ \theta \end{bmatrix}_{spud}$$

Since the x and y direction are symmetrical so equation becomes:

$$\begin{bmatrix} f_x \\ f_y \\ f_z \\ M_\phi \\ M_\theta \\ M_\psi \end{bmatrix} = \frac{EI}{l^3} \begin{bmatrix} 12 & 0 & 0 & 0 & -6l & 0 \\ 0 & 12 & 0 & -6l & 0 & 0 \\ 0 & 0 & 0 & 0 & 0 & 0 \\ 0 & -6l & 0 & 4l^2 & 0 & 0 \\ -6l & 0 & 0 & 0 & 4l^2 & 0 \\ 0 & 0 & 0 & 0 & 0 & 0 \end{bmatrix} \begin{bmatrix} x \\ y \\ z \\ \phi \\ \theta \\ \psi \end{bmatrix}_{spud} \tag{3.32}$$

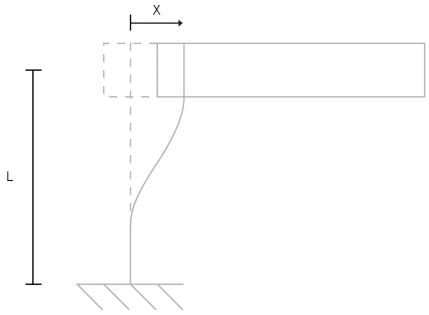

Figure 3.9: ”Displacement of the spud”

Spud K$_{hinge}$ The stiffness matrix of the spud pole when hinging is analyzed in the same fashion and also reference is made to [Wichers1980][6].

$$\begin{bmatrix} f_x \\ f_z \\ M \end{bmatrix} = \underbrace{3 \cdot \frac{EI}{l^3} \begin{bmatrix} 1 & 0 & -l \\ 0 & 0 & 0 \\ -l & 0 & l^2 \end{bmatrix}}_{\overline{\overline{K}}_{spud}} \begin{bmatrix} u \\ w \\ \theta \end{bmatrix}_{spud} \tag{3.33}$$

Numeric values k_{xy} Examples of values of the spud stiffness clamped from direction x resulting in a force in direction y.

$$\begin{aligned} k_{xx} &= 7.6951 \cdot 10^7 \\ k_{yy} &= 7.6951 \cdot 10^7 \end{aligned}$$

3.6.2. Ladder

Cutter head

The last reaction force for the displaced cutter ladder are the soil reaction forces on the cutter head. Damen Dredging Equipment is very experienced in dealing with these forces. When the reaction forces of springs work on the cutterhead. The stiffness of the springs are highly dependant on the soil conditions the dredger is working in. For further purposes a spring stiffness of 600 kN/m is used. Please note that the soil conditions have a large influence on the way that the spud pole is supported. This means that these parameters can not be varied individually.

3.7. Coupling

Hinge

When determining a local stiffness matrix only the translational coefficients have to be considered. Rotations are transformed from the centre of gravity to translations at the hinge location.

$$\begin{bmatrix} K_x & 0 & 0 \\ 0 & K_y & 0 \\ 0 & 0 & K_z \end{bmatrix}$$

The bending of two hinge pins in x and z direction.

$$K_x = K_z = 2 \cdot \frac{48 \cdot EI}{L^3}$$

With

$$I = \frac{\pi}{4} \cdot r^4$$

For y direction the bending of two plates determines the stiffness.

$$K_y = 2 \cdot \frac{3EI}{L^3}$$

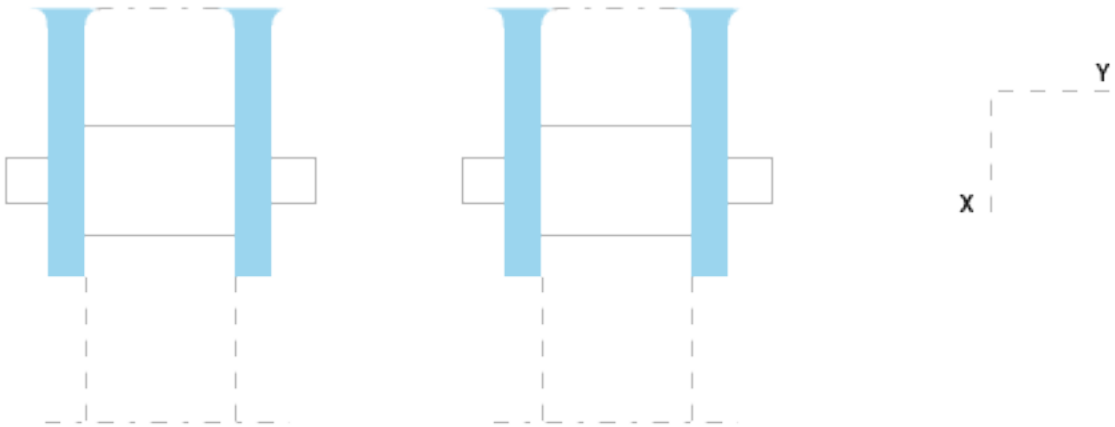

Figure 3.10: ”Ladder hinge”

Hoisting wire

The force that acts on the body's from the hoisting wires is dependant of the elongation of the hoisting wire with respect to its equilibrium length. [4]

$$f_{hw} = \frac{EA}{l_0} \cdot \Delta l \tag{3.34}$$

The relationship between the displacements of the two points of the hoisting wire and the elongation is stated as B=$\overline{B}$

$$\Delta l_{hw} = \overline{B} \cdot \overline{x} = \begin{bmatrix} \cos\alpha & 0 & \sin\alpha & 0_3 & -\cos\alpha & 0 & -\sin\alpha & 0_3 \end{bmatrix} \begin{bmatrix} x_{hwb} \\ y_{hwb} \\ z_{hwb} \\ \phi_{hwb} \\ \theta_{hwb} \\ x_{hwl} \\ y_{hwl} \\ z_{hwl} \\ \phi_{hwl} \\ \theta_{hwl} \\ \psi_{hwl} \end{bmatrix} \tag{3.35}$$

To get the force vector this is the elongation times the elasticity times the normalized direction.

$$\overline{f}_{hw} = \Delta l_{hw} \cdot \frac{EA}{l_0} \cdot \frac{\bar{l}_{hw,0}}{l_0} \tag{3.36}$$

For further notation of the relation of the elongation and force is:

$$\overline{L^{\star}_{hw}} = \frac{EA}{l_0} \cdot \frac{\bar{l}_{hw,0}}{l_0} \tag{3.37}$$

To be able to get the hoisting wire vector a transformation of the x_{ladhwl} that is is the reference frame of the ladder to x_{hwl} that is in the reference frame of the barge.

$$\overline{x}_{hwl} = \overline{x}_{hin} - \overline{x}_{hinlad} + \overline{x}_{ladhwl} \tag{3.38}$$

Then vector of the hoisting wire is:

$$\bar{l}_{hwb} = \bar{x}_{hwb} - \bar{x}_{hwl} \tag{3.39}$$

The elongation of the hoisting wire is the difference between the length of the vector and the original length of the loaded hoisting wire in equilibrium.

$$\Delta l_{hw} = l_{hw} - l_{hw,0} \tag{3.40}$$

Since these displacements are not the displacement in the CoG, transformation matrices are needed.

$$\Delta l_{hw} = \bar{B}\begin{bmatrix}\bar{x}_{hwb}\\ \bar{x}_{hwl}\end{bmatrix} = \bar{B}\begin{bmatrix}\bar{\bar{L}}_{hwbbar} & 0\\ 0 & \bar{\bar{L}}_{hwllad}\end{bmatrix}\begin{bmatrix}\bar{x}_{bar}\\ \bar{x}_{lad}\end{bmatrix} \tag{3.41}$$

$$\bar{f}_{hwl} = \bar{L}^{\star}_{hw}\bar{B}\bar{\bar{L}}_{tot}\bar{x} \tag{3.42}$$

To transform the forces to the CoGs the principle of virtual work is used

$$\delta\bar{x}^{T}_{hw}\bar{f}_{hw} = \delta\bar{x}_{CoG}\bar{f}_{CoG} \tag{3.43}$$

This means that the local virtual work done by the hoisting wire must be the same as the global virtual work. This gives:

$$\delta\bar{x}_{hw}\bar{\bar{f}}_{hw} = \delta\bar{x}^{T}_{hw}\bar{\bar{L}}^{\star}\bar{B}\bar{x} \tag{3.44}$$

$$\delta\bar{\bar{x}^{T}}\bar{\bar{f}}_{CoG} = \delta\bar{\bar{x}^{T}}\bar{\bar{L}}^{T}_{tot}\bar{L}^{\star}_{hw}\bar{B}\bar{\bar{L}}_{tot}\bar{x} \tag{3.45}$$

$$\bar{f}_{CoG} = \bar{\bar{L}}^{T}_{tot}\bar{L}^{\star}_{hw}\bar{B}\bar{\bar{L}}_{tot}\bar{x} \tag{3.46}$$

Due to the assumption of only small rotations, a simplification is made to calculate the forces in the hoisting wire due to its difference in length with respect to its equilibrium length. However, the change in direction of the force is not taken in to account under the assumption that these changes are very small. An highly exaggerated example is show in figure 3.11. The hoisting wire in equilibrium is shown as blue line 1. The elongated wire is shown as 2. The forces acting in situation 2 are drawn as dark blue lines.

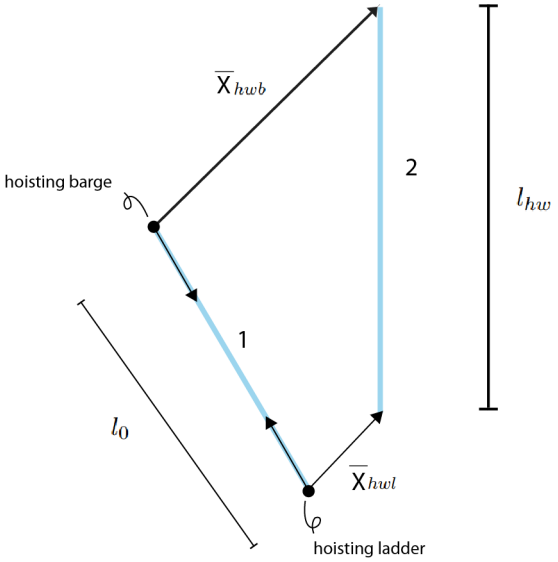

Figure 3.11: "Direction of hoisting wire force"

Steel cables

The hoisting wire of a CSD650 consists of a galvanized stranded steel wire. Due to the fact it is stranded. This means that the steel wire has a reduced elasticity modulus. Where normal steel has an $E = 210 \cdot 10^9 N/mm^2$ for the steel wire this is $105 \cdot 10^9 N/mm^2$[7]. This means that the steel wire stiffness is reduced by a factor 0.5. Not only the Young's modulus is reduced by the stranded wire. Due to fact that a stranded wire consists of multiple steel wire's the cross section of the wire is not completely filled with steel as seen in 3.12. This means that the use of the area of a circle will not suffice. In industry catalogues like [8] a steel wire is described of an outside diameter of $38mm = \pi \cdot \left(\frac{38}{2}\right) = 1134mm^2$ has an effective metallic cross section of 664 mm^2. Reducing the area of an $36mm = 1017mm^2$ with the same factor yields a metallic cross section of $610mm^2$

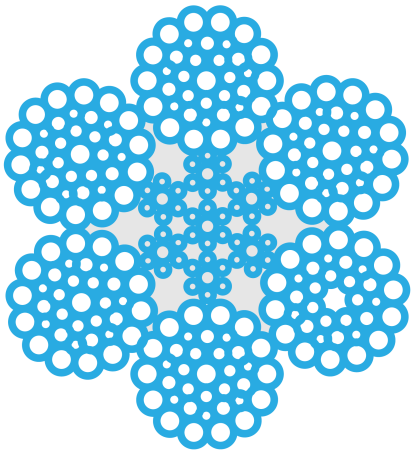

Figure 3.12: "6x36 SW steel core"

3.8. External forces

In this section all the external forces on the system will be discussed. External forces on the system are forces that are not dependent on the acceleration velocity or displacement of the barge or ladder.

3.8.1. Barge

The most important wave force on the barge are the wave forces. These are the forces that are calculated from the undisturbed wave i.e. the Froude-Krylov force. These forces are calculated with diffraction software discussed in section 3.9.

3.8.2. Ladder

To calculate the wave forces on an inclined ladder in waves, for forty different frequencies and twenty for different wave directions the following approach is used:

At first the orbital velocity is calculated for the current water depth 18 m with 3.52. This gives us the horizontal particle velocities over the depth with intervals of 0.1 m. considering that the seabed is flat this particle velocity will be the same for every wave direction. Then velocity in every direction can be decomposed in to a velocity in the x and y direction of the ladder axis system.

$$u_x = \cos\theta \cdot u(wd, \omega) \tag{3.47}$$

$$u_y = \sin\theta \cdot u(wd, \omega) \tag{3.48}$$

Where;

v_x = Particle velocity in x direction
θ = Wavedirection
$v(z, \omega)$ = Particle velocity for over the depth and frequencies

When the x and y velocity's are known, the Morison equation can be used to compute the forces on the ladder can be calculated for every 0.1 m. However the Morison equation in this form is only valid for vertical cylindrical piles. However in the case of an inclined cylinder the cross section in horizontal direction appears to be elliptical. This is why two different diameters must be used when with Morison. For the inertia term the diameter transverse to the flow direction must be used, and for the drag term the diameter parallel to the flow direction must be used.

in x direction
Inertia = D
Drag = D^*

in y direction
Inertia = D^*
Drag = D

Then using the linear Morison equation 3.68. The forces in x and y direction for all the different wave direction and for all the 180 different water depths are known. When summing all these forces over the depth the total force in x and y direction are known.

total force in x direction $\int_{-z}^{z} f_x dz$
total force in y direction $\int_{-z}^{z} f_y dz$
total force in z direction $\int_{-z}^{z} f_z dz$ = always 0

With the distances from every 0.1 segment to the CoG of the ladder known the moments working on the ladder can also be calculated:

total moment about the x axes $\int_{-z}^{z} f_y \cdot |z| dz$
total moment about the y axes $\int_{-z}^{z} f_x \cdot |z| dz$
total moment about the z axes $\int_{-z}^{z} f_y \cdot |x| dz$

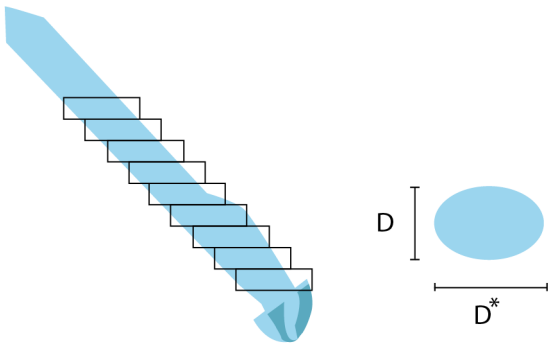

Figure 3.13: "Numerical treatment of the ladder"

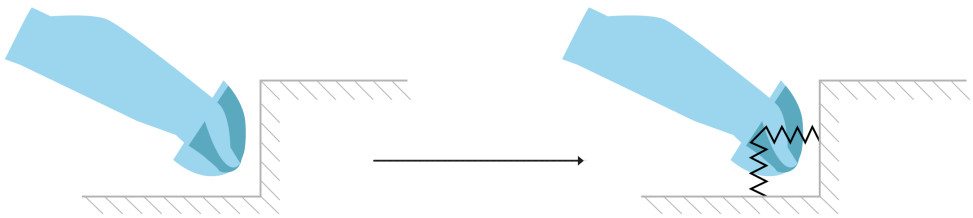

Figure 3.14: "Modeling of the cutterhead reaction forces"

D = The equivalent hydrodynamical diameter = 1.4 m
D^* = $\sin\alpha$
α = Ladder angle

3.9. Diffraction theory

Diffraction theory is used to calculate wave forces on an arbitrarily shaped, fixed or free-floating body. It uses a right-handed, earth bound axis system $S(x_0, y_0, z_0)$ with its origin at the mean water level and z_0 axis vertically upwards. In accordance to linear potential theory, the potential of the dredger is a superposition of the potentials due to the diffraction of the undisturbed incoming wave on the fixed body Φ_d, the potentials due to the undisturbed incoming wave Φ_w and the radiation potentials due to the six body motions Φ_j [2].

$$\Phi = \sum_{j=1}^{6} \Phi_j + \Phi_w + \Phi_d \tag{3.49}$$

The boundary conditions are:

- La place equation
- Sea bed boundary condition
- Free surface boundary condition
- Kinematic boundary condition on the oscillating body surface
- Radiation condition
- Symmetric or anti-symmetric condition

$$\Phi_j(x,y,z) = \frac{1}{4\pi} \iint_{S_0} \sigma_j(x,,) \cdot G(x,y,z,x,,) \cdot dS_0 \tag{3.50}$$

for j = 1,...7

Where:

- $\Phi_j(x,y,z)$ = the potential function on the mean wetted body surface S_0
- $\sigma_j(x,,)$ = is the complex source strength in a point on the mean wetted body surface S_0.
- $G(x,y,z,x,,)$ is the Green's function. Describes the influence of the source $\sigma_j(x,,)$ in a point located at $(x,,)$ on the potential $\Phi_j(x,y,z)$ in a point located at (x,y,z).

3.10. Morison

For hydrodynamic forces on slender vertical tubular structures often the Morison equation is used as follows[2]:

$$F(t) = \frac{1}{2}\rho D C_d \vec{u}(t)|u(t)| + \frac{\pi}{4}\rho D^2 C_M \vec{u}(t) \tag{3.51}$$

With:

ρ = Density of seawater
C_d = Drag coefficient
C_m = Inertia coefficient
D = Diameter
$\vec{x}(t)$ = Particle velocity

As stated in Keuning [1984] [9], schematization of the ladder to a closed, cylindrical construction will be acceptable. If the diameter/wavelength ration does not exceed a value of about 0.15. and the wave height/diameter ratio is less than 1. the diffraction forces become negligible and the

Morison equation can be used. For the cutter ladder an equivalent diameter of 1.4 m is chosen. The minimum wavelength is 15.41 as shown in table 3.2. this ratio does not exceed 0.15.

Although the Morison equation is applicable for all cylindrical structures is does have some limitations:

- Diameter of the cylinder must be much smaller than the wavelength.
- Keulegan–Carpenter numbers
- When extended to orbital flow which is a case of non uni-directional flow, for instance encountered by a horizontal cylinder under waves, the Morison equation does not give a good representation of the forces as a function of time.

3.10.1. Particle velocity

This section considers a still ladder subjected to undisturbed wave forces. the flow velocity around the ladder is determined by the orbital velocity. This flow velocity is calculated with the dispersion equation

According to the velocity potential the amplitude of the flow velocity is[2]:

$$u_x = \omega a \frac{cosh[k(d+z)]}{sinh(kd)} \tag{3.52}$$

$$u_z = \omega a \frac{sinh[k(d+z)]}{sinh(kd)} \tag{3.53}$$

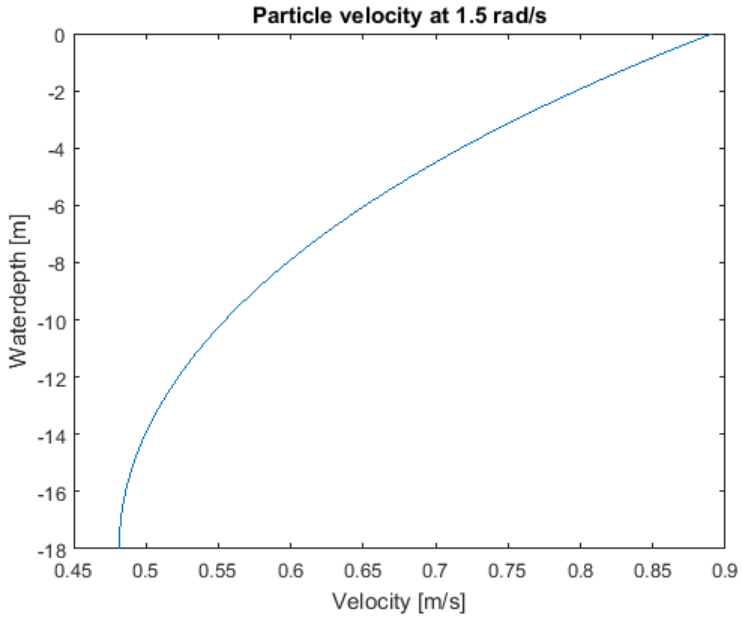

Figure 3.15: "Particle velocity"

With the dispersion equation [10]:

$$\omega^2 = g \cdot k \cdot \tanh kd \tag{3.54}$$

Which must be solved iteratively for each ω. Given a water depth of 18 m and a wave height of 1 m the wavelengths are:

Frequency [rad/s]	Wave number [rad/m]	Wavelength [m]	Wave period [s]
0.05	0.0038	1668.59	125.664
0.10	0.0075	832.38	62.83
0.15	0.0114	552.79	41.89
0.20	0.0152	412.35	31.42
0.25	0.0192	327.58	25.13
0.30	0.0232	270.63	20.94
0.35	0.0274	229.59	17.95
0.40	0.0317	198.48	15.71
0.45	0.0361	174.00	13.96
0.50	0.0408	154.16	12.57
0.55	0.0456	137.70	11.42
0.60	0.0508	123.78	10.47
0.65	0.0562	111.81	9.67
0.70	0.0620	101.39	8.98
0.75	0.0681	92.22	8.38
0.80	0.0747	84.07	7.85
0.85	0.0818	76.79	7.39
0.90	0.0894	70.25	6.98
0.95	0.0976	64.35	6.61
1.00	0.1065	59.02	6.28
1.05	0.1159	54.21	5.98
1.10	0.1260	49.86	5.71
1.15	0.1368	45.93	5.46
1.20	0.1482	42.39	5.24
1.25	0.1603	39.20	5.03
1.30	0.1730	36.33	4.83
1.35	0.1862	33.74	4.65
1.40	0.2001	31.40	4.49
1.45	0.2145	29.29	4.33
1.50	0.2295	27.38	4.19
1.55	0.2450	25.65	4.05
1.60	0.2610	24.07	3.93
1.65	0.2775	22.64	3.81
1.70	0.2946	21.33	3.70
1.75	0.3122	20.13	3.59
1.80	0.3303	19.02	3.49
1.85	0.3489	18.01	3.40
1.90	0.3680	17.07	3.31
1.95	0.3876	16.21	3.22
2.00	0.4077	15.41	3.14

Table 3.2: Frequency Wave number and Wavelength at 18 m water depth

3.10.2. Linear Morison

This form of Morison is not suitable for FD analysis due to the non linearities. But by stating that the linear form must dissipate equal amounts of energy as the linearized form. With power being force times velocity.

$$P_{nl} = F_{nl} \cdot u \tag{3.55}$$

Using the the nonlinear drag force,

$$F_{nl} = \frac{1}{2}\rho D C_d u|u| \tag{3.56}$$

Substituting in to equation 3.55

$$P_{nl} = \frac{1}{2}\rho D C_d \cdot u^2|u| \tag{3.57}$$

The linear drag force is:

$$F_{lin} = C_{lin} \cdot u \tag{3.58}$$

with C_{lin} to be determined and multiplied with the velocity to get the power.

$$P_{lin} = C_{lin} \cdot u^2 \tag{3.59}$$

with the particle velocity over time

$$u = u_a \cos \omega t \tag{3.60}$$

The dissipated energy must be the same over an entire period.

$$\int_0^{2\pi} P_{nl}\,\mathrm{d}t = \int_0^{2\pi} P_{lin}\,\mathrm{d}t \tag{3.61}$$

is

$$\int_0^{2\pi} \frac{1}{2}\rho D C_d u_a \cos \omega t |u_a \cos \omega t| \cos \omega t\,\mathrm{d}t = \int_0^{2\pi} C_{lin} \cdot u_a \cos^2 \omega t\,\mathrm{d}t \tag{3.62}$$

$$\int_0^{2\pi} \cos \omega t |\cos \omega t| \cos \omega t\,\mathrm{d}t = \frac{3}{8} \tag{3.63}$$

$$\int_0^{2\pi} \cos^2 \omega t\,\mathrm{d}t = \pi \tag{3.64}$$

using the result of 3.64 and 3.63

$$\frac{1}{2}\rho D C_d u_a^3 \frac{3}{8} = u_a^2 C_{lin} \pi \tag{3.65}$$

$$C_{lin} = \frac{1}{2}\rho D C_d \frac{3}{8\pi} u_a \tag{3.66}$$

Substitute in equation 3.62 to get the

$$F_{drag}(t) = \frac{1}{2}\rho D C_d [\frac{8}{3\pi} u_a] \cdot u \tag{3.67}$$

The total linearised drag force becomes.

$$\vec{F}_{lin}(t) = \frac{1}{2}\rho D C_d [\frac{8}{3\pi} u_a] \cdot u + \frac{\pi}{4}\rho D^2 C_M u \tag{3.68}$$

This is confirmed in literature for example in [11]

3.10.3. Phase

To incorporate the forces in the model correctly the phase differences between the wave forces on the centre of gravity of the barge and the centre of gravity of the ladder must be known. To calculate them the following steps are undertaken.

- First the distance between the CoG of the barge and the CoG of the ladder projected on the flow direction must be known. For example this will be the full distance for waves in 0 and 180 degrees and will be 0 for the waves from 90 and 270 degrees.
- Then for every frequency that has its own wavelength see tabular 3.2. That wavelength corresponds to a full 2π phase.
- After that every wavelength must be divided by the distance between the CoGs for that wave direction.
- The important part of that division is the number after the decimal sign. When this number is multiplied by 2π the phase difference between the CoG of the barge and ladder is known.

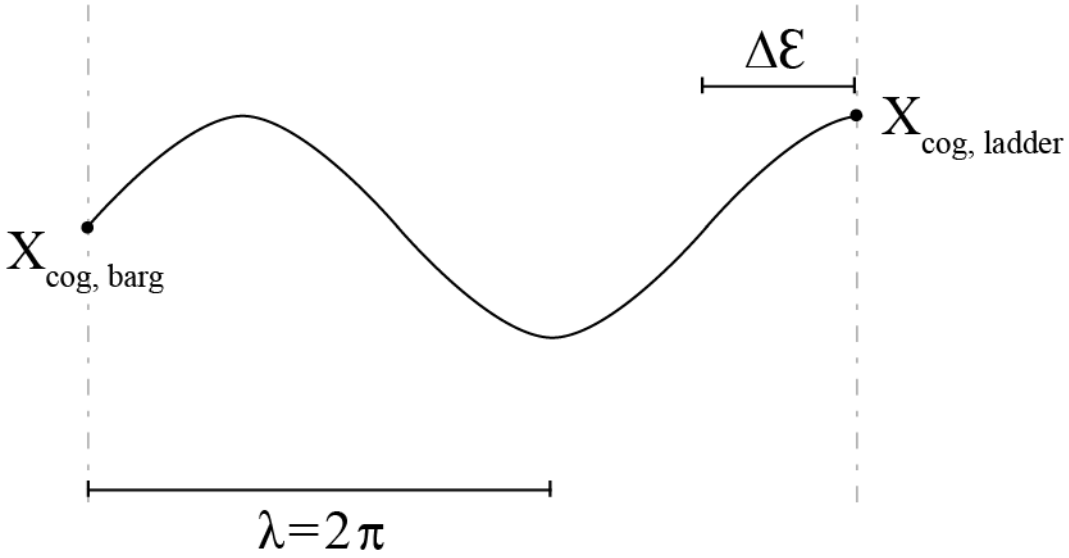

Figure 3.16: ”Calculating the phase difference”

4

Algorithm and Implementation

In chapter 3 all the forces on the CSD are discussed. All the information to fill in the complete equation of motion are in place and all further calculation steps to answer the research questions are discussed in the following chapter.

4.1. Equation of motion

The total equation of motion now becomes: Cummins[1962] [12]: [13]

$$\begin{vmatrix} M_b + A_{\omega,b} & 0 \\ 0 & M_l + A_{\omega,l} \end{vmatrix} \begin{vmatrix} \ddot{\bar{x}}_b \\ \ddot{\bar{x}}_l \end{vmatrix} + \begin{vmatrix} K_{hyd} + K_{spu} + K_{hin,bb} + K_{hoi,bb} & K_{hin,bl} + K_{hoi,bl} \\ K_{hin,lb} + K_{hoi,lb} & K_{cut} + K_{hin,ll} + K_{hoi,ll} \end{vmatrix} \begin{vmatrix} \bar{x}_b \\ \bar{x}_l \end{vmatrix} = \begin{vmatrix} F_{wave,b,\omega} & 0 \\ 0 & F_{wave,l,\omega} \end{vmatrix} - F_{retardation} \tag{4.1}$$

and in frequency domain (FD)

$$\left\{ -\omega^2 \cdot \begin{vmatrix} M_b + A_{\omega,b} & 0 \\ 0 & M_l + A_{\omega,l} \end{vmatrix} + i\omega \cdot \begin{vmatrix} B_{\omega,b} & 0 \\ 0 & B_{\omega,l} \end{vmatrix} + \begin{vmatrix} K_{hyd} + K_{spu} + K_{hin,bb} + K_{hoi,bb} & K_{hin,bl} + K_{hoi,bl} \\ K_{hin,lb} + K_{hoi,lb} & K_{cut} + K_{hin,ll} + K_{hoi,ll} \end{vmatrix} \right\} \begin{vmatrix} \bar{X}_b \\ \bar{X}_l \end{vmatrix} = \begin{vmatrix} F_{wave,b,\omega} & 0 \\ 0 & F_{wave,l,\omega} \end{vmatrix} \tag{4.2}$$

4.2. Frequency domain

In only one degree of freedom the FD analysis goes as follows:

$$[k - \omega^2 m + i\omega b]X = H_{fz}Z \tag{4.3}$$

Giving

$$\frac{F(s)}{X(s)} = -\omega^2(M + A) + i\omega(B + B_{visc}) + K \tag{4.4}$$

This ratio is a so called transfer function, it gives the ratio between the incoming wave height and the resulting force. When for every frequency and in every direction the transfer function is known, the wave elevation can be multiplied with the transfer function for that frequency.

$$\frac{X_{CoG}}{Z} = \frac{H_{FZ}(\alpha, \omega)}{-\omega^2(M + A(\omega)) + i\omega(B(\omega) + B_{visc}) + K_{sys}} \tag{4.5}$$

$$F(\omega, t) = (M + A(\omega))\ddot{x} + (B(\omega) + B_{visc})\dot{x}(t) + Kx(t) \tag{4.6}$$

$$\ddot{x}(t) = \frac{F(t) - (B(\omega) + B_{visc})\dot{x}(t) + Kx(t)}{M + A(\omega)} \tag{4.7}$$

4.3. Stress in spud pole

When the motions of the CoG are determined in the FD analysis the stresses in the spud pole can be calculated. First the motions of the CoG $\overline{x}_{CoG}$ must be transformed to motion in the spud pole $\overline{x}_{spu}$ by means of the transformation matrix $\overline{\overline{L}}_{sc}$.

$$\overline{x}_{spu} = \overline{\overline{L}}_{sc}\overline{x}_{CoG} \tag{4.8}$$

When the motions of the spud barge at the spud pole are known, the relation between spud motions and maximum stress in the spud is needed.

The maximum stress in the out most fibre of the spud pole is:

$$\sigma_{zz} = \frac{M \cdot r}{I} \tag{4.9}$$

The moment in the spud pole in lateral direction when assuming a clamped spud pole is caused by a lateral force and a moment from the barge to the spud pole. These are related as followes:

For the rotation:

$$\phi = \frac{M \cdot l}{EI} + \frac{Fl^2}{2 \cdot EI} \tag{4.10}$$

and the translation:

$$x = \frac{M \cdot l^2}{2 \cdot EI} + \frac{Fl^3}{3 \cdot EI} \tag{4.11}$$

$$\theta \cdot \frac{2 \cdot EI}{l} = M + FL \tag{4.12}$$

$$x \cdot \frac{6 \cdot EI}{l^2} = 3 \cdot M + 2 \cdot FL \tag{4.13}$$

Since the max moment in the spud is caused by $F * l$ and M.

$$M_{yy} = x \cdot \frac{6 \cdot EI}{5 \cdot l^2} + \theta \cdot \frac{EI}{l} \tag{4.14}$$

and

$$M_{xx} = y \cdot \frac{6 \cdot EI}{5 \cdot l^2} + \phi \cdot \frac{EI}{l} \tag{4.15}$$

$$M_{yy} = RAO_x \cdot \frac{6 \cdot EI}{5 \cdot l^2} + RAO_\theta \cdot \frac{EI}{l} \tag{4.16}$$

and

$$M_{xx} = RAO_y \cdot \frac{6 \cdot EI}{5 \cdot l^2} + RAO_\phi \cdot \frac{EI}{l} \tag{4.17}$$

in vector matrix notation this gives:

$$M_{yy} = \begin{bmatrix} \frac{6 \cdot EI}{5 \cdot l^2} & 0 & 0 & 0 & \frac{EI}{l} & 0 \end{bmatrix} \begin{bmatrix} x \\ y \\ z \\ \phi \\ \theta \\ \psi \end{bmatrix}_{spud} \tag{4.18}$$

for transversal direction:

$$M_{xx} = \begin{bmatrix} 0 & \frac{6 \cdot EI}{5 \cdot l^2} & 0 & \frac{EI}{l} & 0 & 0 \end{bmatrix} \begin{bmatrix} x \\ y \\ z \\ \phi \\ \theta \\ \psi \end{bmatrix}_{spud} \tag{4.19}$$

The moment in the spud pole in lateral direction assuming the spud pole is hinged in the soil:

Substituting the moments into equation 4.9 gives $H_{\sigma,lat}$ or $H_{\sigma,trans}$ the relation between the motions of the spud cage and the maximum stress in the spud pole. However the stress in lateral and transversal direction are not of a lot of interest. Most important is the maximum stress over the entire cross section of the spud pole 4.1.

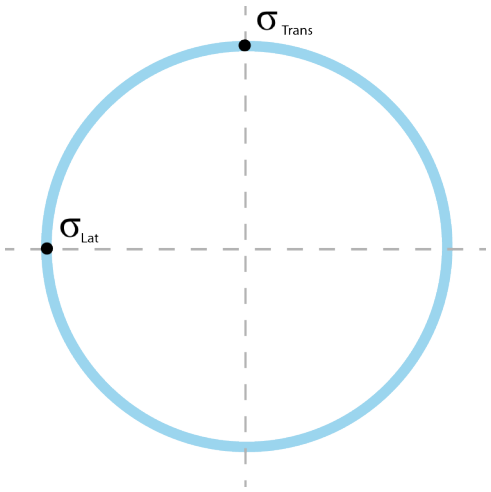

Figure 4.1: "Stress in spudpole"

Hinging spud pole

For the hinging example a different relation between the motions and moments is needed. The relation between the motion and maximum moment is different. The bending moment is derived by using the local stiffness matrix in 3.33.

$$M_{yy} = \begin{bmatrix} \frac{3 \cdot EI}{l^2} & 0 & 0 & 0 & -\frac{3EI}{l} & 0 \end{bmatrix} \begin{bmatrix} x \\ y \\ z \\ \phi \\ \theta \\ \psi \end{bmatrix}_{spud} \tag{4.20}$$

symbol		dimensions	for
H_fz	=	[6x1]	ω,α
L_{spubar}	=	[6x6]	
A_ω,B_ω	=	[6x6]	ω
M,K	=	[6x6]	
$H_{\sigma,spud}$	=	[2x6]	
$H_{\sigma,M}$	=	[2x6]	
$K_{spud,loc}$	=	[6x6]	

for transversal direction

$$M_{xx} = \begin{bmatrix} 0 & \frac{3 \cdot EI}{l^2} & 0 & -\frac{EI}{l} & 0 & 0 \end{bmatrix} \begin{bmatrix} x \\ y \\ z \\ \phi \\ \theta \\ \psi \end{bmatrix}_{spud} \tag{4.21}$$

4.4. Stress response amplitude operators

Using Σ_{tans} for the σ in frequency domain, everything needed to get to so called spud stress RAO:

$$\frac{\Sigma_{bend}}{Z} = \frac{H_{\sigma,spu} L_{spubar} H_{FZ}(\alpha,\omega)}{-\omega^2(M + A(\omega)) + i\omega(B(\omega) + B_{visc}) + K_{sys}} \tag{4.22}$$

$$H_{\sigma,spud} = H_{\sigma,M} \cdot K_{spud,loc} \tag{4.23}$$

$$H_{\sigma spu} = \begin{bmatrix} \sigma_{bend,I} \\ \sigma_{bend,II} \end{bmatrix} = \begin{bmatrix} 0 & 0 & 0 & \frac{D*0.5}{I_{xx}} & 0 & 0 \\ 0 & 0 & 0 & 0 & \frac{D*0.5}{I_{yy}} & 0 \end{bmatrix} \tag{4.24}$$

4.5. Wave spectrum

For further analysis of the behavior of a CSD in waves a wave spectrum must be given. For the purpose of this thesis the JONSWAP spectrum is chosen. However in the model any given wave spectrum can be chosen.[2]

$$S_\zeta(\omega) = \frac{320 \cdot H_{1/3}^2}{T_p^4} \cdot \omega^{-5} \cdot exp\left\{\frac{-1950}{T_p^4} \cdot \omega^{-4}\right\} \cdot \gamma^A \tag{4.25}$$

4.6. Stress spectrum

If we want to devise the stress spectrum for a particular part of the CSD we first need the spectra for each motion. To get to these, the wave spectrum $S_z(\omega)$ and the the response amplitude operators are needed. These RAOs are calculated using equation 4.5. For example the motion spectrum of heave is calculated as [2]:

$$S_\zeta(\omega) \cdot d\omega = \frac{1}{2}\zeta_a^2(\omega) \tag{4.26}$$

from a wave spectrum to a heave spectrum:

$$S_z(\omega) \cdot d\omega = \frac{1}{2}z_a^2(\omega) \tag{4.27}$$

$$S_z \cdot d\omega = |\frac{z_a}{\zeta_a}(\omega)| \cdot \frac{1}{2}\zeta_a^2(\omega) \tag{4.28}$$

$$S_z \cdot d\omega = |\frac{z_a}{\zeta_a}(\omega)| \cdot S_\zeta(\omega) \cdot d\omega \tag{4.29}$$

$$S_z(\omega) = RAO_z^2 \cdot S_z(\omega) \tag{4.30}$$

By multiplying the spectral wave height by the square of the unit response at the same frequency, we get $m^2 sec$ plotting these for the full range of frequencies we get the particular motion spectrum[14]. Since the relation between motions and stress in the spud pole is calculated in 4.22 stress spectrum can be devised resulting in 4.31.

$$S_\Sigma = RAO_\Sigma^2 \cdot S_z(\omega) \tag{4.31}$$

4.7. Yield stress Exceedance

Within the frequency domain it is not possible to calculate the maximum stress in the spud pole during a certain time with constant sea state. However it is possible to calculate the chance of exceeding a certain stress value from the stress spectrum. This method is analogue to the calculation of the wave crest exceedance chance described by Holthuijsen [2007] [10].

$$P\{\eta_{crest} > \eta\} = \frac{\overline{f_\eta}}{\overline{f_0}} = exp\left(-\frac{\eta^2}{2m_0}\right) \tag{4.32}$$

Equation 4.32 calculates the probability of one wave crest being higher than a certain threshold value under the assumption of a Reighley distribution of the wavelength. With □is the threshold value and m_0 the zeroth spectral moment of the wave spectrum. Assuming the stress response has the same Reighley distribution the same steps can be done for the stress spectra. In equation 4.33 the threshold value σ_y is the yield stress of the steel. Stresses higher will lead to plastic deformation.

$$P\{\sigma > \sigma_y\} = \frac{\overline{f_{\sigma_y}}}{\overline{f_0}} = exp\left(-\frac{\sigma_y^2}{2m_0}\right) \tag{4.33}$$

$$f_0 = \frac{1}{2\pi}\sqrt{\frac{M_2}{M_0}} \tag{4.34}$$

To get the yield stress exceedance probability not only the exceedance probability of one single stress cycle must be known. The number of stress cycles within a period of time is needed. This is the cycle frequency and is calculated according to Holthuijsen [2007] [10] in equation 4.34. To calculate the total YSEP for a certain period of time the probabilities of each individual cycle can be superimposed as in equation 4.35

$$P_{fail} = T_d \cdot f_0 \cdot P\{\sigma > \sigma_y\} \tag{4.35}$$

4.8. Fatigue

Fatigue is the progressive, localized and permanent structural change that occurs ins a material subjected to repeated or fluctuating strains at nominal stresses that have maximum values less than (and often much less than) the tensile strength of the material. Fatigue may culminate into crack and cause fracture after a sufficient number of fluctuations. [15]

4.8.1. S-N Curves

When the results of fatigue tests are plotted as the stress amplitude S versus the number of cycles, N to fracture. The resulting curve plotted through data points is called an S-N curve[15]. The data is obtained by subjecting smooth or notched specimens to a certain cyclic stress. At first cyclic stresses with high peak stresses near the yield stress are applied. With these high peak stresses failure is expected in a short number of cycles. The stress is decreased until the specimens can reach 10^7 cycles. The stress at witch this first occurs is called the fatigue limit. An example of a S-N curve is shown in figure 4.2 from [16].

Low cylce	0.5	<	N	≤	10^3
Medium cycle	10^3	<	N	≤	10^5
High cycle	10^5	<	N	≤	10^7

Table 4.1: Cycle ranges

The NEN-EN 1993-1-9 norm [17] gives the SN curves for welded steel members as shown in figure 4.2. The horizontal axis shows the number of cycles on a logarithmic scale. The vertical axis shows the stress range. The numbers on the lines indicate which line to use for different welds and structure types.

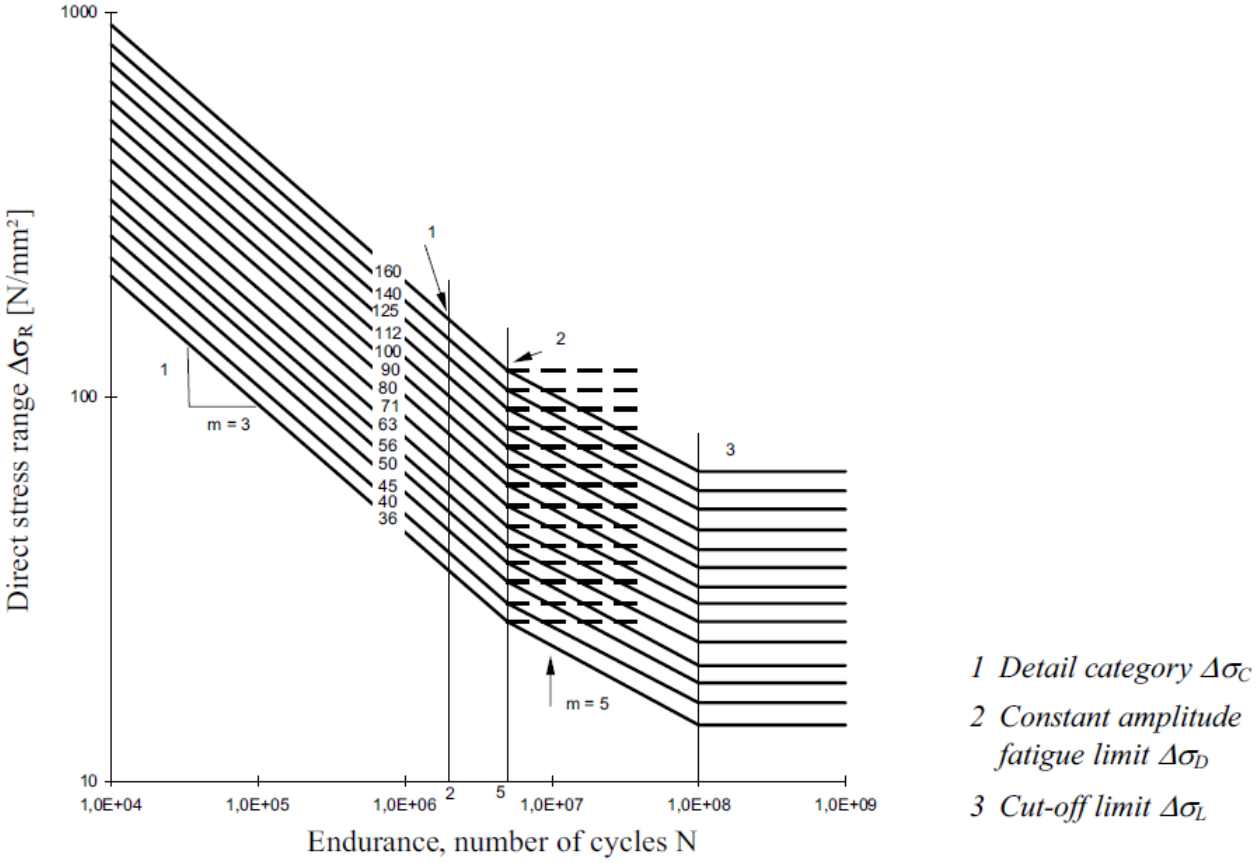

Figure 4.2: "SN Curves for fatigue of steel structures"

To get a structure specific SN Curve the detail category $\Delta\sigma_C$ and K_s are needed.

$$\Delta\sigma_{C,red} = K_s \Delta\sigma_C \tag{4.36}$$

Table 8.3 of the NEN gives for a transverse butt welds welded from one side the detail category of 71 and a size effect for t > 25 mm.

$$K_s = \left(\frac{25}{t}\right)^{0.2} \tag{4.37}$$

The NEN norm gives for the constant amplitude fatigue limit $\Delta\sigma D$ and for the cut off limit of $N_L = 2e^6$ at $\Delta\sigma_L$.

$$\Delta\sigma_D = \left(\frac{2}{5}\right)^{\frac{1}{3}} \Delta\sigma_C = 0.737\Delta\sigma_C \tag{4.38}$$

and

$$\Delta\sigma_L = \left(\frac{5}{100}\right)^{\frac{1}{5}} \Delta\sigma_D = 0.549\Delta\sigma_D \tag{4.39}$$

For stress spectra with stress ranges above and below the constant amplitude fatigue limit $\Delta\sigma_D$ the fatigue strength should be bases don the extended fatigue strength curve:

$$\Delta\sigma_R^m N_R = \Delta\sigma_C^m \cdot 2 \cdot 10^6 \tag{4.40}$$

with m = 3 for $5 \cdot 10^6 \geq$ N

$$\Delta\sigma_R^m N_R = \Delta\sigma_D^m \cdot 5 \cdot 10^6 \tag{4.41}$$

with m = 5 for $10^8 \geq$ N $\geq 5 \cdot 10^6$

In comparison with the normal SN curve formula which is:

$$N = K \cdot S^{-m} \tag{4.42}$$

This gives values of:

$$K = \Delta\sigma_c^m \cdot 2 \cdot 10^6 \tag{4.43}$$

with m = 3 for $5 \cdot 10^6 \geq$ N

$$K = \Delta\sigma_D^m \cdot 5 \cdot 10^6 \tag{4.44}$$

with m = 5 for $10^8 \geq$ N $\geq 5 \cdot 10^6$

4.8.2. Long term stress distribution

Since the relationship between the wave height and stress is known as in section 4.3. This transfer function $H_\sigma(\omega)$ can be used to calculate the stress spectrum of the spud pole. This stress spectrum $S(\omega)$ can be obtained as found in Bai[2003] [18]:

$$S(\omega) = |H_\sigma(\omega)|^2 \cdot S_\eta(\omega) \tag{4.45}$$

The n^{th} spectral moment of this stress response is:

$$m_n = \int_0^\infty \omega^n \cdot S_\sigma(\omega)\,\mathrm{d}\omega \tag{4.46}$$

The average stress cycle period is thus:

$$T_0 = 2\pi\sqrt{\frac{m_0}{m_2}} \tag{4.47}$$

Nonlinear effects due to large amplitude motions and large waves can be neglected in the fatigue assessment since the stress ranges at lower load levels contribute relatively more to the cumulative fatigue damage. In cases where linearization is required, it is recommended that the linearization is performed at a load level representative of the stress ranges that contribute the most to fatigue damage, i.e. stresses at probability levels of exceedance between 10^{-2} to 10^{-4}. The stress range response may be assumed to be Rayleigh distributed within each sea state as:

$$F(S) = 1 - exp\left(-\frac{S^2}{8m_0}\right) \tag{4.48}$$

4.8.3. Miner's rule

A structural part is subjected to a variable amplitude load is subjected to fatigue. The structural is at his percentage of fatigue lifetime according to the Miner's rule [19]:

$$\sum \frac{n_i}{N_i} = 1 \tag{4.49}$$

In which

n_i = Number of cycles of stress level i
N_i = Number of cycles of stress level i that leads to failure

This rule can be applied to the stress spectrum created for the stress amplitude in the spud pole. To get a idea of how much of the fatigue lifetime a spud pole has used we first take a look at the stress spectrum. At every frequency band the stress spectrum has a certain stress value. For every stress value the number of cycles until most probable failure of that stress range can be determined through the corresponding SN curve. These values can be used in the denominator of the Miner's rule. However for the numerator part the number of cycles within the chosen time span is not known. These number of cycles can be determined using the dispersion equation. Every frequency has its own period at a certain water depth. If this period of every stress is known in second, divided by the time span of the certain sea state and wave direction in seconds. This is how the number of cycles of every frequency is determined. When over a certain period of time all the factors of the Miner's rule can be summed up to get the factor of the fatigue lifetime the spud has used.

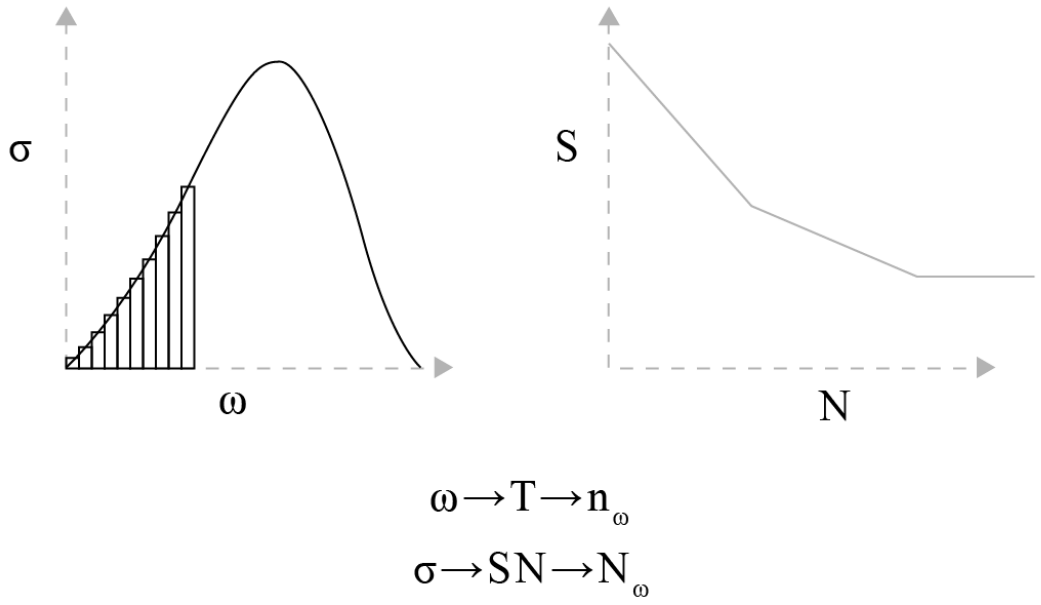

Figure 4.3: "Using the Miner's rule"

4.8.4. Fatigue damage calculation

Following the Miner's rule, the accumulated damage of a sea state may be expressed in the continuous form.

$$D_{fat} = \int_0^{\infty} \frac{n(S)}{N(S)} dS \tag{4.50}$$

Where $n(S)dS$ represents the number of stress ranges between S and S+dS. If a stationary response process of duration T_{life} is assumed, the total number of stress cycles will be:

$$n(S)dS = \nu_{0i} T_{life} p(S)dS \tag{4.51}$$

The average frequency of response will be:

$$\nu_{0i} = \frac{1}{2\pi}\sqrt{\frac{m_{2i}}{m_{0i}}} \tag{4.52}$$

The total short term fatigue damage calculation becomes:

$$D_{fat} = \nu_{0i} T_{life} \int_0^\infty \frac{p(S)}{N(S)} ds = \frac{\nu_{0i} T_{life}}{K} \int \frac{S^{(m+1)}}{4\sigma_i^2} exp(-\frac{S^2}{8\sigma_i^2}) ds \tag{4.53}$$

$$\Gamma(1+\frac{m}{2}) = \int_0^\infty e^{-x} x^{\frac{m}{2}} dx \tag{4.54}$$

$$D_{fat} = \frac{\nu_{0i} T_{life}}{K} \cdot (8m_{0i})^{\frac{m}{2}} \cdot \Gamma(1+\frac{m}{2}) \tag{4.55}$$

4.8.5. Wave scatter

Where the wave spectrum provides a short term description of the sea state. The wave scatter provides a long term description in figure 4.4 an example is shown.

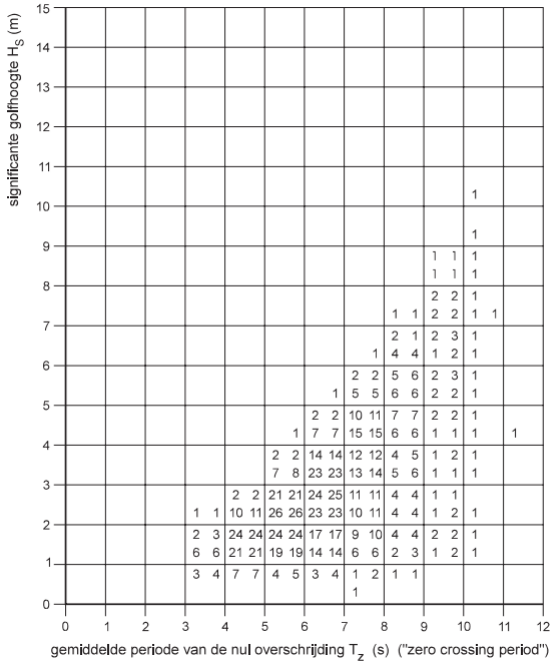

Figure 4.4: "Wave scatter for the North-sea"

For a whole year at a certain interval the significant wave height and the average zero up crossing period is measured at a location. The vertical axes shows the significant wave heights from 0 to 11 m. The horizontal axes gives the average zero crossing period from 0 to 12 seconds. At every combination of wave height and period a number is shown. This number corresponds with at how many intervals this combination is measured in parts per thousand. This gives a good view of the wave climate of that location in one year.

However the values H_s and T_p are input variables for the JONSWAP wave spectrum. Assuming a wave buoy did a thousand measurements in the course of a year. With 8760 hours in a year and we assume that the sea state is the same between each measurement. Roughly one can state that the wave climate remains the same over the course of 9 hours. Section 4.8.4 covers the calculation of the fatigue damage over one wave spectrum. Adding all these fatigue damages gives the fatigue damage over one year for a working dredger. However a CSD will only be work in 60 % of the time. And during significant wave heights higher than H_s the dredger will not operate.

4.8.6. Long term fatigue damage calculation

To be able to calculate the long term fatigue damage the long term sea states have to be known. This is for example done with a wave scatter diagram discussed in section 4.8.5. This wave diagram gives the number of occurrences of a certain sea state defined by a significant wave height and a period. Using all these wave heights and periods for every type of sea state a JONSWAP spectrum can be generated. Using the methods discussed in section 4.5. For every sea state a stress spectra and by extension zeroth and second order moments of these sea states. To combine the these different stress spectra's, moments and the fatigue characteristics of the spud pole. Reference is made to the DNV notes 30.7. Fatigue assessment of ship structures. There a fatigue damage calculation is proposed incorporating all these factors:

$$N = K \cdot S^{-m} \tag{4.56}$$

$$\begin{aligned} D = v_0 T_d \sum_{i=1,j=1} r_{ij} \left(\frac{(2\sqrt{2M_{0ijn}})^{m_1}}{K_1} \right) \Gamma\left(1 + \frac{m_1}{2}; \left(\frac{S_0}{2\sqrt{2M_{0ijn}}} \right)^2 \right) \\ + \left(\frac{(2\sqrt{2m_{0ijn}})^{m_2}}{K_2} \right) \gamma\left(1 + \frac{m_2}{2}; \left(\frac{S_0}{2\sqrt{2m_{0ijn}}} \right)^2 \right) \end{aligned} \tag{4.57}$$

$$\begin{aligned} D = f_0 \cdot T_d \cdot \left(\frac{(2\sqrt{2M_0})^{m_1}}{K_1} \right) \Gamma\left(1 + \frac{m_1}{2}; \left(\frac{S_0}{2\sqrt{2M_0}} \right)^2 \right) \\ + \left(\frac{(2\sqrt{2M_0})^{m_2}}{K_2} \right) \gamma\left(1 + \frac{m_2}{2}; \left(\frac{S_0}{2\sqrt{2M_0}} \right)^2 \right) \end{aligned} \tag{4.58}$$

Equation 4.58 incorporates three different aspects of fatigue at once.

- The long term wave statistics represented by the wave scatter diagram
  - p_{ij} = Chance of occurrence sea state i j.
  - v_{ij} = $\frac{1}{2\pi}\sqrt{\frac{M_{2ij}}{M_{0ij}}}$ Response zero crossing frequency for sea state i j.
  - v_0 = $\sum p_{ij} \cdot v_{ij}$ Long term average zero crossing frequency.
  - r_{ij} = $\frac{v_{ij}}{v_0}$ Relative number of stress cycles in short term condition.
- The short term response of the sea states represented by the zeroth spectral moment.
  - $M_0 = \int_0^\infty \omega^0 \cdot S_\sigma(\omega) d\omega$
  - $M_2 = \int_0^\infty \omega^2 \cdot S_\sigma(\omega) d\omega$
- And the SN curve of the welded spud pole represented by the K_1, K_2, a_1 and a_2.

5

Runs and Results

To be able to understand why and how the spud poles fail it is necessary to look at the two most important failure mechanisms yield stress and fatigue. Therefore the calculation methods discussed in chapter 4 are used. In this chapter all the results of these calculation are shown.

First the wave forces that are the DELFRAC input are shown, then the motion RAOs of the barge are discussed. These are the result of solving the equation of motion in the frequency domain. These motions can be translated to the motion of the spud cage. From there the stress in the spud pole as a consequence of the motions.

In section 5.4 the stress spectra are presented from which further statistical analyses can be done. From these stress spectra the probability of yield stress is calculated 5.5. In practice the user of a CSD650 would like to know what the probabilities of failure are of the spud pole within every sea state.

The users can now decide in what sea states they will allow their dredger to operate. However the stress cycles under the yield stress may not permanently deform the spud pole but do inflict a certain damage to the spud pole this damage is calculated in section . Unless stated otherwise the characteristics of the runs are set to the following:

- Ladder angle 45 degrees
- Water depth 18 m
- wave spectrum JONSWAP H_s = 1 m T_p = 6 s
- Normal stiffness spud pole EI = $2.7 \cdot 10^6\ kNm^2$

5.1. Wave forces

The wave forces on the barge in the six degrees of freedom are shown in figure 5.1. These are the addition of the Froude-Krylov and diffraction forces. [20]. Please note that wave forces are cyclic and the figure shows the amplitudes for different frequencies.

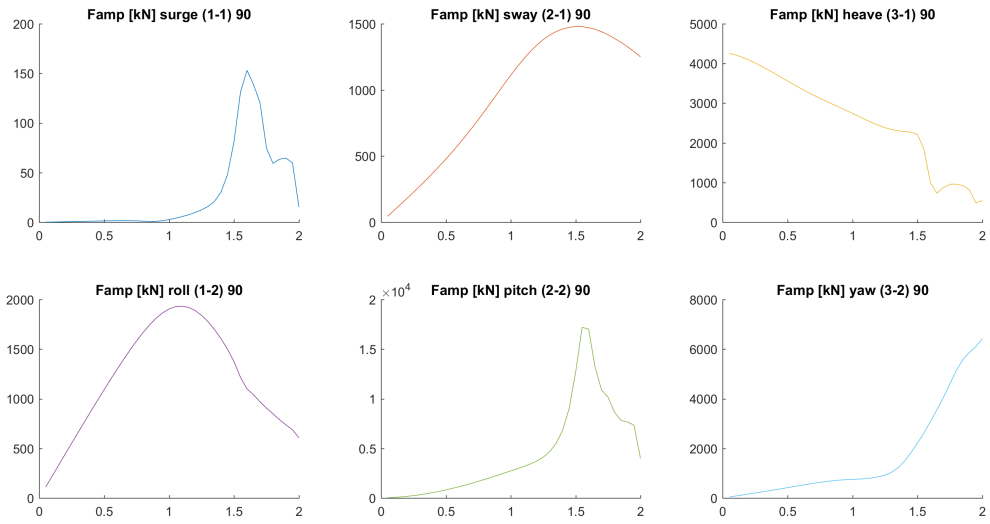

Figure 5.1: "Waver forces calculated by DELFRAC"

5.1.1. Verification

To verify these results with easy to do formulas we can calculate the Froude-Krylof wave force. The Froude–Krylov force does, together with the diffraction force, make up the total non-viscous forces acting on a floating body in regular waves. The diffraction force is due to the floating body disturbing the waves. [21]. The pressure pf a undisturbed wave on a object in finite water depth is according to [Journee] [2]:

$$\rho \cdot g \cdot \zeta \cdot \frac{\cosh k(h+z)}{\sinh k \cdot h} \cdot \cos xk - \omega t \tag{5.1}$$

h = water depth
k = wave number
z = vertical distance of the concidered point below mean water level
ω = radial frequency
ρ = density of water
g = gravitational acceleration
ζ = wave height

Since we want to know the force subjected on the body we must calculate the difference between the pressure on the front an at the back. At t=0 and for x = length of the ship we get the amplitude of the FK force equation 5.2

$$\frac{FK}{\zeta} = D \cdot B\rho \cdot g \cdot \frac{\cosh k(h+z)}{\sinh k \cdot h} \cdot \cos xk \tag{5.2}$$

The results of the calculations are shown in figure 5.4. For comparison the results of the wave forces determined with DELFRAC are shown.

5.2. Motion RAOs

One of the most important graphs are the response amplitude operators. In figure 5.2 six graphs are shown representing the six motions of the barge. On the horizontal axes the 40 different frequencies are shown in radians per second. On the vertical axes the 24 wave directions from 0 to 360 degrees are shown.

Table 5.1: "Barge RAO's wavedir 180 degrees"

DOF\Omega [rad/s]	0.25	0.5	0.75	1	1.25	1.5
1	0.58	1.30	2.39	2.65	0.32	0.18
2	0.01	0.08	0.01	0.00	0.00	0.00
3	0.96	0.82	0.54	0.11	0.09	0.06
4	0.00	0.01	0.00	0.00	0.00	0.00
5	0.02	0.05	0.07	0.06	0.01	0.00
6	0.00	0.01	0.00	0.00	0.00	0.00

The first thing that strikes are the amplitudes of the sway and yaw motions at low frequencies. Due to these spikes the scaling of the plots does not show any more information. These spikes are probably caused by high wave forces at wave directions of 270 and 90 degrees. However when limiting the upper color boundary to 10 more information in the rest of the plot becomes visible 5.2.

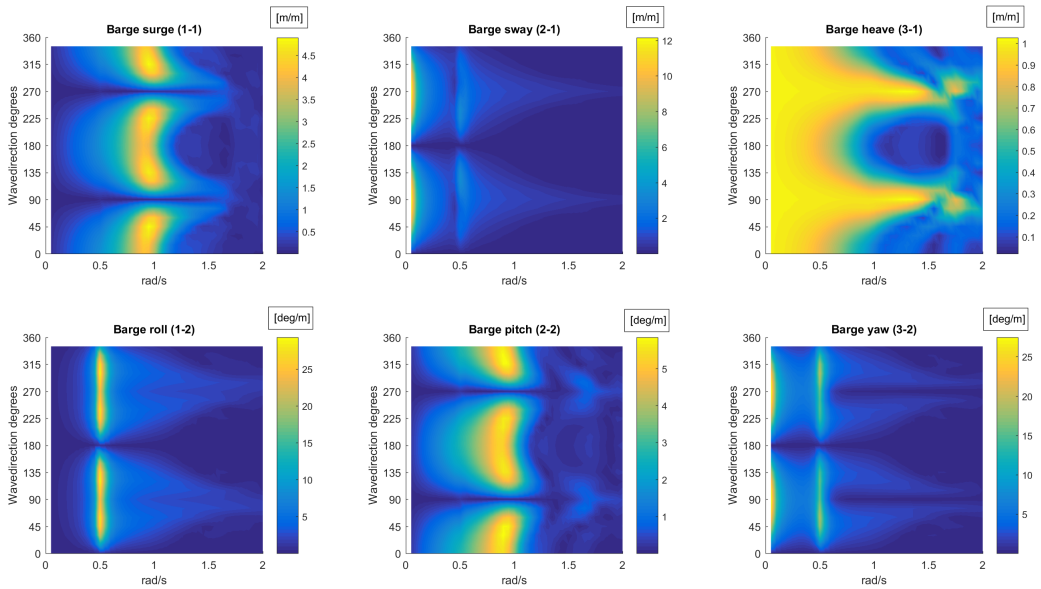

Figure 5.2: "Barge RAO"

Now the RAOs of the centre of gravity of the barge are known. It is translated to the motions of centre of the spud cage with a transformation matrix discussed in 3.3.1. The only difference between the RAOs of the barge and the spud is found in the heave motions in figure 5.3. This is because only the x coordinate of the spud cage differs significantly from that of the CoG. $(x, y, z) = (0, 0, 0) - (-25.5, 0, -0.6)$. This means that only the heave motion will be amplified by the distance.

5.2.1. Verification

To verify that the model is a representation of the CSD650 some simple verification checks can be done.

- surge
  - Surge should be maximum at wave direction 0 or 180
  - Surge should be 0 at wave direction 90 or 270
- sway

  - Sway should be 0 at wave direction 0 or 180
  - Sway should be maximum at wave direction 90 or 270
- heave
  - Heave should be 0 at high frequencies
  - Heave should be 1 at low frequencies
  -
- roll
  - Should be maximum when at the wave direction 90 and 270.
  - and maximum at which the wavelength corresponds with half the width of the ship. The maximum is at 1.7 rad/s ant this is about 20m.
- pitch
  - Should be maximum at wave direction 180.
  - Should be maximum when wavelength corresponds with half the length. The maximum is at about 0.6 rad per second and corresponds with 120 m.

This list applies to the RAOs of the barge CoG in figure 5.2.

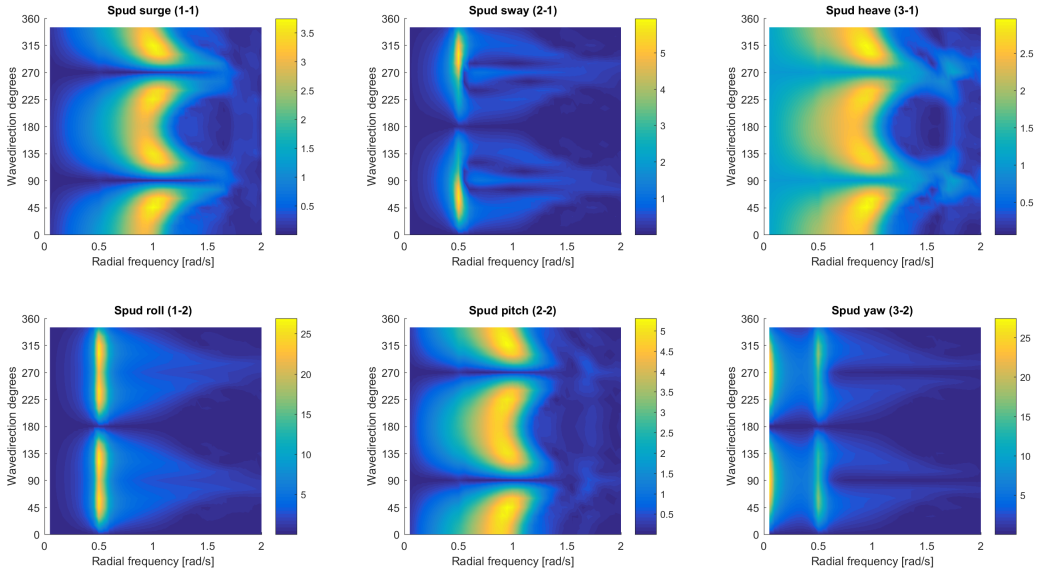

Figure 5.3: ”RAO of the spud cage”

Some simple checks can also help to verify the calculation method, in figure 5.4 in the top graph, three different motions are shown over the frequencies. First is the blue line representing the horizontal amplitude of the motion of a water particle in a unit wave. The orange line represents a one degree of freedom system in surge direction with normal spud stiffness but without any damping. Due to the fact that there is no damping the eigenfrequency is clearly visible around the 1.3 rad/s. The yellow line is the surge RAO of the 6 DOF system with the coefficients calculated by DELFRAC.

$$\frac{X}{\zeta} = \frac{\frac{FK}{\zeta}}{k_{spu} - \omega^2(m+a)} \tag{5.3}$$

With

$m + a$ = $m \cdot 1.15$
k_{spu} = $\frac{3*EI}{h^3}$
$\frac{FK}{\zeta}$ = From equation 5.2

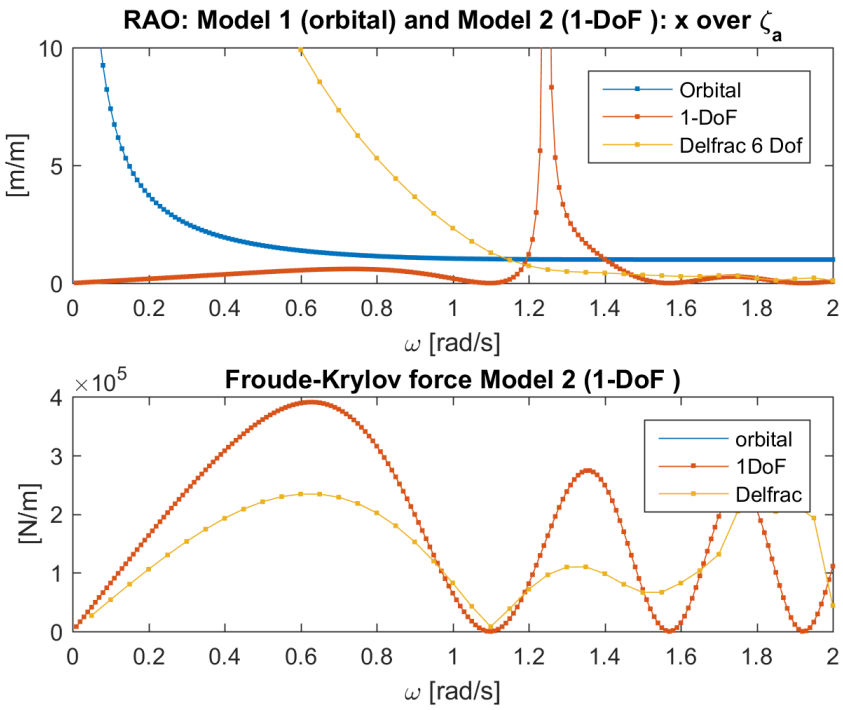

Figure 5.4: ”wave force calculations”

5.3. Stress responses

Now the motions of the spud cage are known we can establish the link between these motions and the stresses in the spud pole. This link is discussed in 4.3. The RAO shown in figure 5.5 represents the amplitude response function of incoming waves for different frequencies and wave directions and the stress amplitude in the spud pole in y direction. The peak of the stress amplitude is easily recognised at about 0.5 rad/s and a wave direction of 45, 135 and 225, 315 degrees. In these wave directions the contributions of roll and sway are the largest.

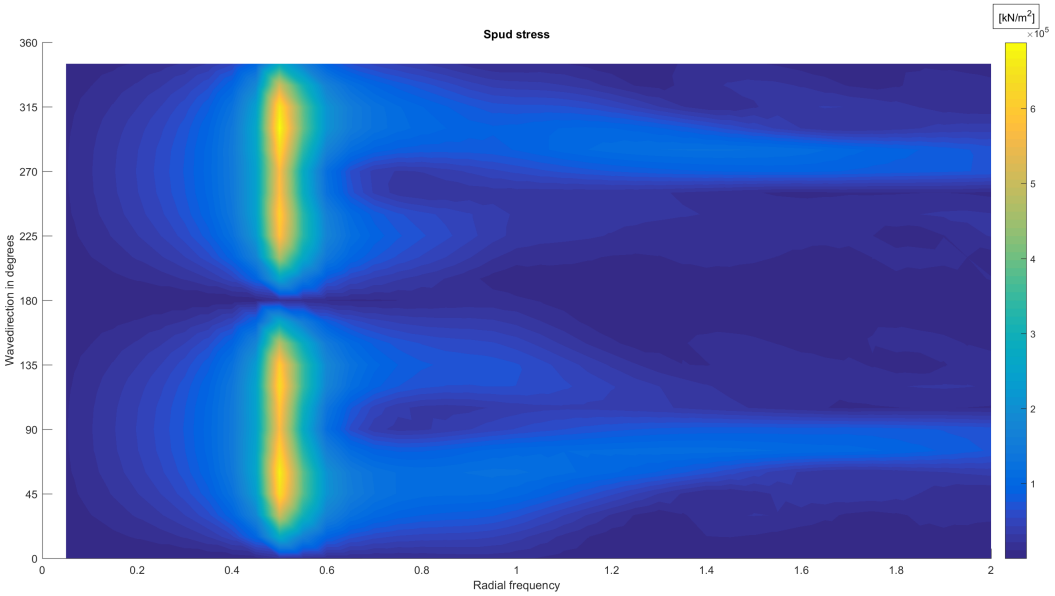

Figure 5.5: ”Spud Stress RAOs in y direction”

To put these amplitudes in perspective the amplitudes are divided by the yield stress of the used construction steel 355 N/mm^2. In figure 5.7 it is clear that the maximum stress in the spud pole due to regular waves in the steady state is nearly half the yield stress of the steel.

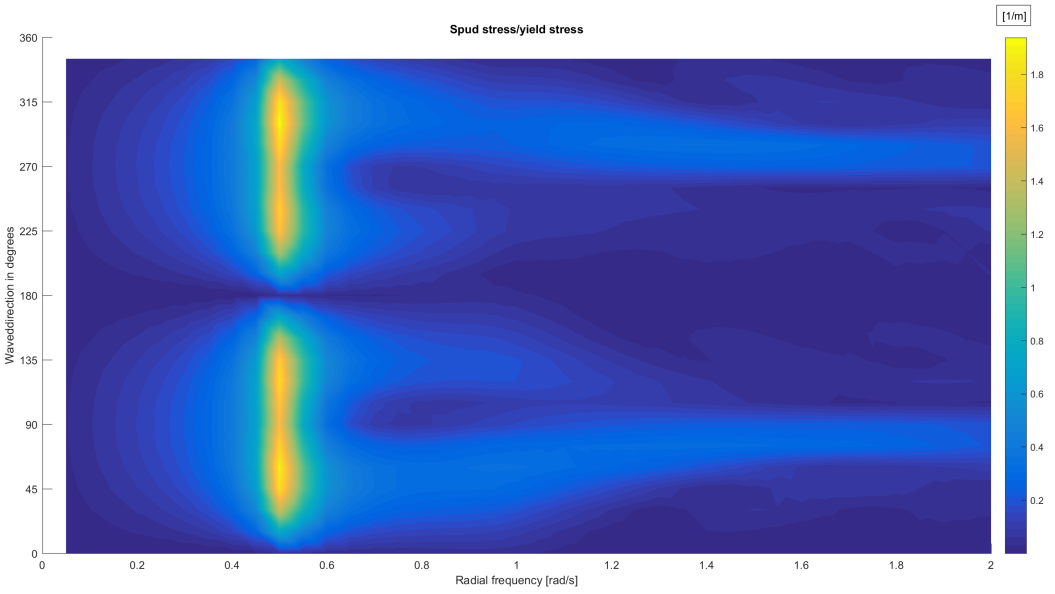

Figure 5.6: ”Factorised Spud Stress RAOs in y direction”

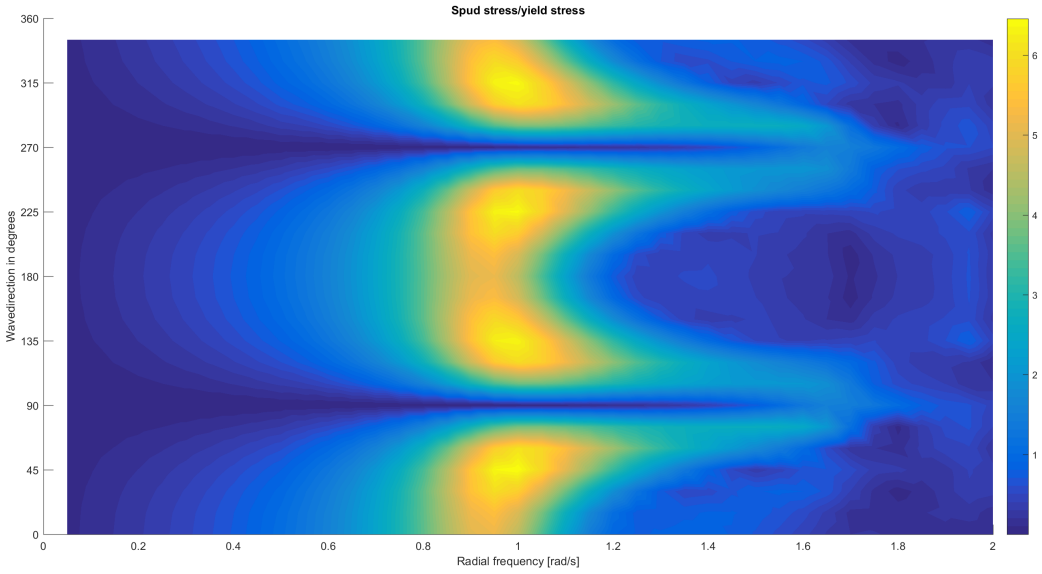

Figure 5.7: "Factorised Spud Stress RAOs in x direction"

5.4. Spectrum

The waves to which the CSD are subjected in this model are assumed to be of the JONSWAP spectrum. This spectrum is treated in section 4.5. It is easy to see that the peak lies at a slightly higher frequency than 1 rad/s. This corresponds with a period of 6 seconds through the dispersion equation see 3.2

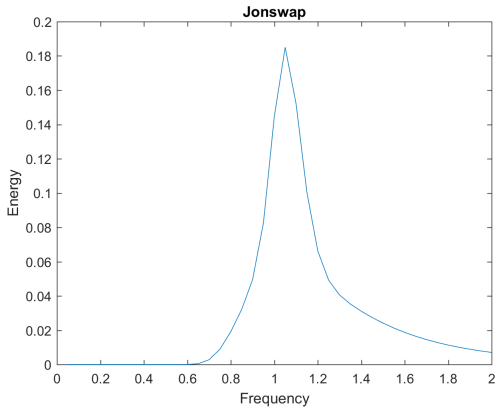

Figure 5.8: "JONSWAP spectrum for 1 m H_s 6 sec T_p"

Combining the wave spectra and the stress RAOs as explained in section 4.6. Striking is that the peak of the stress spectra are a lot higher that the yield stress of the construction steel. In Figure 5.9. The stress spectra of the first twelve wave directions are shown.

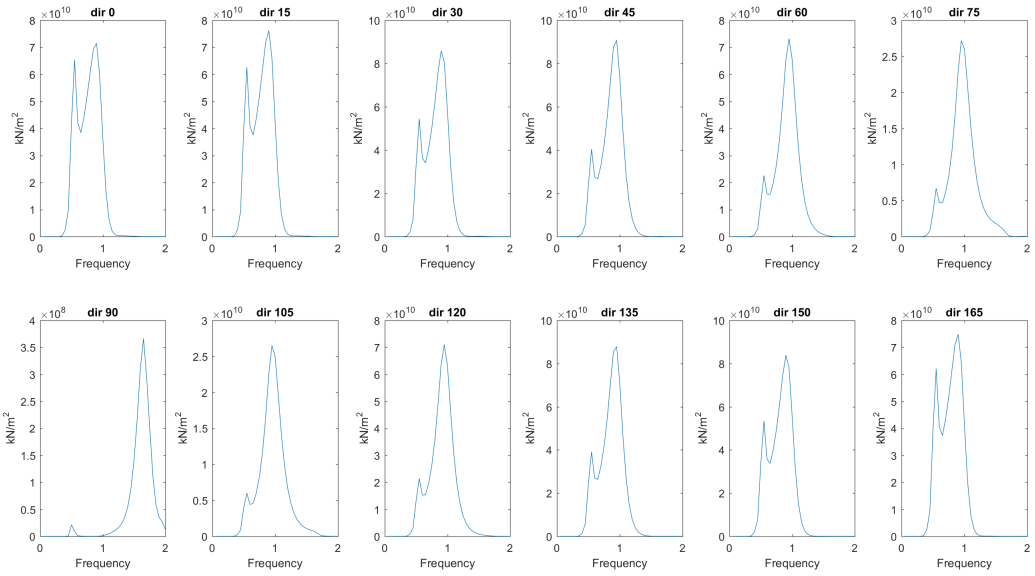

Figure 5.9: "Stress spectrum for the first 12 wave directions"

5.5. Yield stress exceedance

With these stress spectra, a lot of information about the stress response is available using the method described in section **??**. This is the probability that the amplitude of one response cycle exceeds the yield stress. To be able to calculate the exceedance probability in 3 hours, the frequency of a response cycle is needed.

$$P\{\sigma > \sigma_y\} = \frac{\overline{f_{\sigma_y}}}{\overline{f_0}} = exp\left(-\frac{\sigma_y^2}{2m_0} \right) \tag{5.4}$$

for example a wave spectrum with the following:

H_s	=	0.5 m
T_p	=	4 s
Wave direction	=	180 degrees
σ_y	=	355 kN/mm

This gives a probability of 0.82 that the stress response is higher than the yield stress and the spud pole will fail due to plastic deformation for every cycle. To calculate the number of stress cycle during a 3 hour sea state we need equation 5.5

$$\overline{f}_0 = \sqrt{\left(\frac{M_2}{M_0} \right)} = 0.1249 \tag{5.5}$$

A frequency of about a 8 seconds for every cycle is twice the peak period of 4 seconds. With a 3 hours weather condition (10800 seconds) this would mean about 1350 cycles. The total probability of exceeding the yield stress would then be $1.96 \cdot 10^5$ percent. This is not a satisfactory result and probably not true. It would be unacceptable for normal use of the CSD650. For normal use of the CSD650 users are looking for probability of yield stress exceedance of around a value of 10^{-4}.

However looking at the dispersion equation a 8 seconds period the wavelength is about 84 meters. This is 24 longer than the ships length and should not be causing these high YSEP.

To get insight in which sea states cause the most probability of exceeding the yield stress, the calculations are done for a range of sea states. It is easy to see that a higher wave height will lead to higher wave forces and YSEP. In figure 5.10 it is visible that the highest YSEP is near the sea states with an average peak period of 3 seconds.

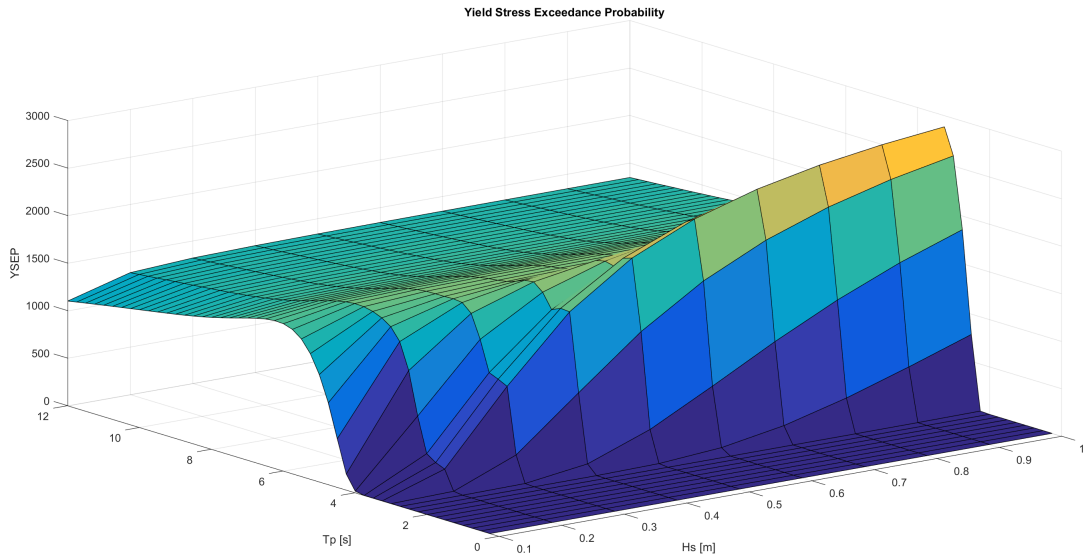

Figure 5.10: "Yield Stress Exceedance Probability in x direction"

These results suggest that the dredger can be used in all sea states ranging up to 3.5 m T_p. In the sea states up to 1 m H_s the average peak periods larger than 3 seconds should be avoided.

5.6. Fatigue

In this section a fatigue analysis is done with all the available information possible. First the fatigue resistance of the spud pole against cyclic stresses must be discusses in section5.6.1. Then the current industry to predict fatigue damage using spectral analysis on specific sea state in section 5.6.2.

5.6.1. SN curve

To determine the proper fatigue resistance for the spud pole of the cutter suction dredger use is made of SN curves. these SN curves are documented in Eurocode 3: Design of steel structures - Part 1-9: Fatigue [17]. In this document SN curves are given for different types of welds.

Detail category	Constructional detail	Description	Requirements
112	size effect for t>25mm: $k_s=(25/t)^{0,2}$ 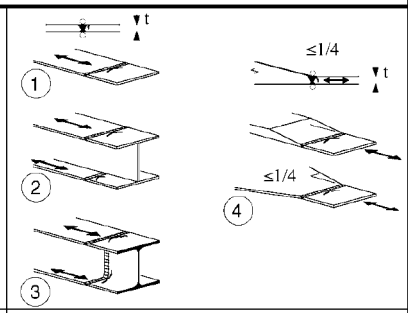	Without backing bar: 1) Transverse splices in plates and flats. 2) Flange and web splices in plate girders before assembly. 3) Full cross-section butt welds of rolled sections without cope holes. 4) Transverse splices in plates or flats tapered in width or in thickness, with a slope ≤ ¼.	- All welds ground flush to plate surface parallel to direction of the arrow. - Weld run-on and run-off pieces to be used and subsequently removed, plate edges to be ground flush in direction of stress. - Welded from both sides; checked by NDT. Detail 3): Applies only to joints of rolled sections, cut and rewelded.

Figure 5.11: "Table 8.3 of NEN 1993 1-9 transverse butt welds"

The butt welded segments of the spud pole have a detail category of 112. This 112 corresponds to the $\Delta\sigma_c$ of equation 4.40 and equation 4.41. However to use these SN curves for the fatigue calculation described in the DNV classification notes no. 30.7 [22]. Since the thickness of the spud pole is smaller than 25 mm no size effect is added.

$$\log N = \log a - m \log \Delta\sigma \tag{5.6}$$

Comparing equations 4.40, equation 4.41 with equation 5.6:

$$a_1 = 112^3 \cdot 10^6 \tag{5.7}$$
$$a_2 = 112^5 \cdot 10^6 \tag{5.8}$$

5.6.2. Short term fatigue calculation

The short term fatigue calculations are based on the Miner's rule for variable amplitude loading. Combining this with the bi-linear SN curve and the stress spectrum equation in equation 4.55. In the following example short term fatigue calculations will be done for one sea state that lasts 3 hours:

for example a wave spectrum with the following

H_s = 0.5 m
T_p = 6 s
Wave direction = 180 degrees
σ_y = 355 kN/mm

This gives a fatigue damage of $1.85 \cdot 10^7$. Since a fatigue damage 1 is considered completely damaged and a 90 % probability of failure [16], it seems that this sea state is very sensitive to fatigue damage. However this result is expected. From earlier results it can be seen that in this sea state the yield stress of the spud pole will be exceeded. When this happens the fatigue damage is accumulated in only one cycle.

for H_s = 1 m
T_p = 4 s

This gives a fatigue damage of $1.27 \cdot 10^3$. However one can argue how often this type of sea state is seen in practice. In figure 5.12 the 3 hour fatigue damage of different sea states are shown surrounding the most common sea states in the North sea as seen coastal working conditions of the CSD650.

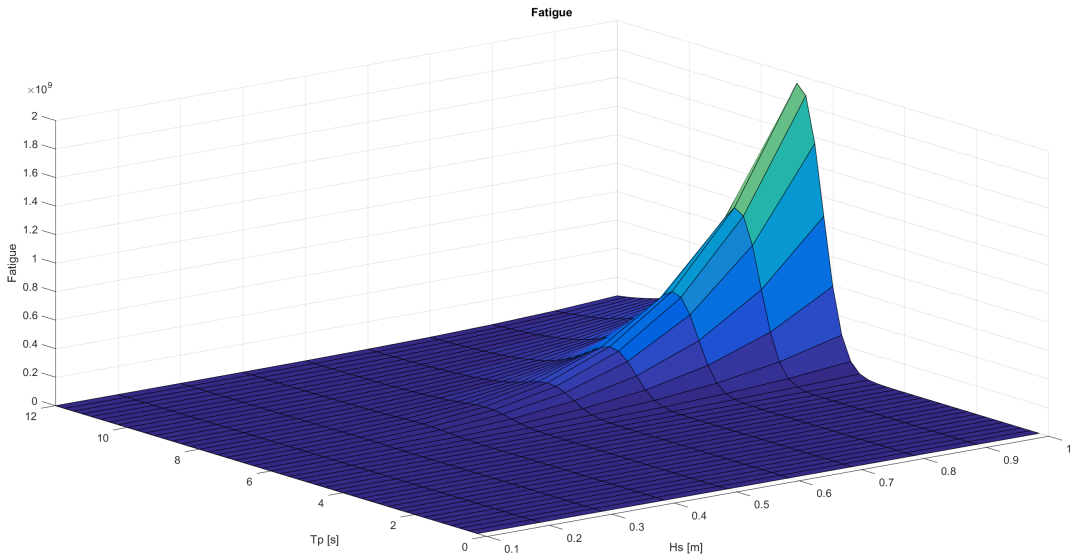

Figure 5.12: "Fatigue Damage"

5.7. Varying spud stiffness

In this section the effect of spud stiffness is investigated. First a description of the intermediate steps that change will discussed and after that intermediate results are shown. When the Stiffness of the spud pole of the system is reduced with a factor 2. In the equation of motion described in

First the effect of the spud flexibility is investigated on the probability of yield stress exceedance adn fatigue. Calculating the over a 3 hours sea state with a stiffness ranging from 0.25 of the normal

EI up to 100 % of the normal EI. These are done for Hs = 0.5 m and Tp = 6 sec.

EI factor	0.25	0.5	0.75	1
P_{exc}	$1.4 \cdot 10^3$	$1.5 \cdot 10^3$	$1.7 \cdot 10^3$	$1.7 \cdot 10^3$
D_{fat}	$4.3 \cdot 10^3$	$1.2 \cdot 10^6$	$1.85 \cdot 10^7$	$9.86 \cdot 10^6$

Table 5.2: ”probability of exceedance for varying EI”

6

Conclusions and Recommendations

6.1. Conclusion

Looking at the results of section 5 the behavior of the CSD can be calculated by a frequency domain model. Even if this means that all non linearities must be neglected or linearised. When accepting a failure probability of 1 of the spud pole by yield stress exceedance. The operational limits of the CSD650 are according to the frequency domain model are that the dredger should not operate in sea states with longer wave periods than about 2.5 seconds.

These are very limiting conditions and are hardly seen in coastal conditions like the North sea, according to the frequency domain analysis and assessment of the fatigue life using SN curves as in the NEN documents, the sea states that cause the most damage are the wave spectra with periods from 7 until 9 seconds. These periods cause stress cycles with high stress amplitudes and 'hurt' the spud pole the most. When looking at stiffness or flexibility of the spud pole the model predicts that a more flexible spud pole leads to significant longer fatigue life. However this will affect the spud poles ability to control the position of the CSD.

6.2. Discussion

Following the results in chapter 5 and the conclusions in section 6.1 it seems that the model overestimates the yield stress exceedance probability and fatigue damage within one sea state. In normal practice Damen Dredging Engineering advises its clients not to use the CSD650 in sea states with waves higher than 0.8 meter.

The model shows that a during a JONSWAP sea state with H_s of 0.8 and a 6 seconds period, the spud pole would probably fail due to fatigue within one stress cycle and would be plastic deformed. The model seems to be able to predict the operational limits to a very precise wave height. However the wave height is not measured very accurately and even more important, not predicted very accurately.

Furthermore, the model assumes that the spud pole is fully clamped in the spud cage. However this is not completely true. The spud cage is almost 2 cm wider than the outer diameter of the spud pole. This means the stress in the spud pole will be showing non linear behavior. This behavior is impossible to incorporate in the frequency domain model. One of the assumptions is, that the spud pole is fully clamped in the soil. However this is not necessarily true. Only in the case of very deep penetration of the spud pole in the soil will this be approximated. In normal practice, the spud can act as anything ranging from a hinge to fully clamped. This changes the place and amplitude of the maximum bending moment in the spud pole and therefore the operational limits and fatigue damage. In the model the forces from the cutterhead of the dredger are incorporated in the equation of motion by adding a spring term in the x and z direction.

However, cutter forces appear to be highly non linear when operating [6]. For the long term fatigue damage the only wave scatter shown in this report is a wave scatter on a location in the North sea with unknown water depth. Nevertheless, it is important to note that waves are influenced by water depth.

Since the CSD650 will only operate in limited water depth it is essential to select an appropriate wave scatter diagram.

6.3. Recommendation

Following the discussion of section 6.2 there is still a lot of research needed. It is important to be able to validate the model with real life measurements. Adding stress gauges at key locations of the spud pole, the stresses measured from these gauges could give stress spectrum of the spud pole over longer periods of time. Furthermore information about failing spud poles in practice would be of great help understanding more about how and why they fail.

Combining this data with wave measurements and comparison with this model would give more insight in the validation of the model and the fatigue damage of the spud pole. Also, the validity of the cutterhead forces being modeled as a reaction of spring force must be investigated.

Finally, implementation in MATLAB has proven to be complex and arduous increasing possible errors. It is likely that the large overestimation of the YSEP and fatigue damage is caused by either programming or implementation errors. Countless efforts are made to check and verify the working of the model. However within the time frame of this thesis, the writer was unable to eliminate them all.

Bibliography

[1] A. W. society, *Standard Welding Terms and Defenitions,* (2010).

[2] J. Journée and W. W. Massie, *Offshore hydromechanics,* (2001).

[3] E. T. Whittaker, *A Treatise on the Analytical Dynamics of Particles and Rigid Bodies,* (1904).

[4] C. Hartsuijker, *Evenwicht,* (1997).

[5] S. Chakrabarti, *Emperical calculation of roll damping for ships and barges,* (2001).

[6] J. Wichers, *Forces on a Cutter suction dredger in waves,* 9th world dredging conference (1980).

[7] staalkabel bv., *Technisch Vademecum,* (1995).

[8] bridon, *Oil and Gas Catalogue,* (2013).

[9] P. Keuning and J. Journée, *calculation method for the behaviour of a cutter suction dredge operating in irregular waves,* (1984).

[10] L. Holthuijsen, *Waves in Oceanic and Coastal Waters,* (2007).

[11] R. van 't Veer, *Application of Linearized Morison Load in Pipe Lay Stinger Design,* (2008).

[12] W. E. Cummins, *The impulse response function and ship motions,* (1962).

[13] O. T, F, *Understanding Cummins Equation.* (1964).

[14] W. H. Michel, *Sea Spectra Simplified,* (1968).

[15] B. Boardman, *Fatigue Resistance of Steels,* (1990).

[16] dr. ing. Dieter Radaj, *Design and Analysis of Fatigue Resistant Welded Structures,* (1990).

[17] NEN, *Design of steel structures Part 1-9: Fatigue,* (1993).

[18] Y. Bai, *Marine Structures Design,* (2003).

[19] J. Schijve, *Fatigue of Structures and Materials,* (2010).

[20] O. Faltinsen, *Sea Loads on Ships and Offshore Structures,* (1990).

[21] O. M. Faltinsen, *Sea Loads on Ships and Offshore Structures,* (1990).

[22] DNV, *Fatigue Assesment of Ship Structures,* (2014).